ISBN 0-315-54890-8

Canada

THE UNIVERSITY OF MANITOBA

FREE OSCILLATIONS OF TWO CONDUCTING SPHERES

by

Richard J. Epp

A THESIS

SUBMITTED TO THE FACULTY OF GRADUATE STUDIES

IN PARTIAL FULFILLMENT OF THE REQUIREMENTS FOR THE DEGREE

OF MASTER OF SCIENCE

DEPARTMENT OF ELECTRICAL ENGINEERING

WINNIPEG, MANITOBA

JUNE 1989

FREE OSCILLATIONS OF TWO CONDUCTING SPHERES

BY

RICHARD J. EPP

A thesis submitted to the Faculty of Graduate Studies of
the University of Manitoba in partial fulfillment of the requirements
of the degree of

MASTER OF SCIENCE

ABSTRACT

The free oscillations of the perfectly conducting two-sphere geometry are determined analytically for large sphere separation. That is, asymptotic expressions for the natural frequencies and natural modes are obtained, correct to first order in inverse sphere separation. Denoting the sphere radii as a and b, we consider all cases $a = b$, $a \neq b$, and $b = 0$, with detailed interpretation of the results.

It is understood that for single-body geometries a free oscillation sustains itself (except for radiation damping) without sources by currents at all locations interacting causally via fields with each other, under constraints imposed by the continuity equation, and of course the boundary conditions. A two-body geometry gave us the unique opportunity to treat each body as a local part of a single "distributed body" to examine this feedback mechanism in detail, and thereby establish a direct and logical link between a natural mode and its corresponding natural frequency, with special emphasis on causality.

We present a theory which links the natural frequencies and natural modes with those of the single-sphere geometry. There appear to be features unique to the two-body geometry, for example a basic duplicity in the expected number of free oscillations, as well as some "anomalous" free oscillations, which are accounted for by suggesting new physical mechanisms.

Although the detailed results are valid only for large sphere separation, this does not seriously limit the goals of this thesis. Most of the ideas and physical insight apply for all sphere separations, and represent necessary reading before tackling the problem by intensely numerical means.

ACKNOWLEDGEMENTS

I wish to thank Dr. L. Shafai for believing in me and allowing me the freedom to choose my own path, which taught me many unique and valuable lessons for life. His patience through many path changes, experience, and constant encouragement are greatly appreciated.

I would also like to thank Wendy for her support and sacrifices, and my friends and colleagues, especially Hamid Moheb for much helpful advice.

The financial assistances provided by the Natural Sciences and Engineering Research Council of Canada and the Department of Electrical Engineering of the University of Manitoba are also greatly appreciated.

Richard Epp

TABLE OF CONTENTS

LIST OF FIGURES

CHAPTER 1: INTRODUCTION

The singularity expansion method (SEM) was introduced by Baum [5] as a means of more fully understanding transient electromagnetic scattering phenomena. Basically, the bilateral Laplace transform of the electromagnetic scattering response contains singularities attributed to both the excitation (waveform singularities) and the scattering body itself (object singularities), which characterize its time domain and complex frequency domain (s-plane) behavior [4]. In particular, Marin [15] has shown that for perfectly conducting finite-size objects in free space the object response has only poles as singularities in the finite s-plane (a meromorphic function). It may also be singular at infinity (the addition of an entire function). Application of the inverse Laplace transform yields the time domain response which, by the Cauchy residue theorem, is a sum of exponentially damped sinusoids (for first order poles), plus contributions from an entire function if present (integration at infinity).

The locations of the poles in the s-plane are called natural frequencies; at these complex frequencies the object can sustain a response without a forcing function. Alternatively, if forced at such a frequency the object will have an infinite response. The corresponding field distributions are called natural modes. A natural mode is a solution of the source free field equations in the presence of the scattering body, that is, satisfying the appropriate boundary conditions, with suppressed time dependence governed by its respective natural frequency. A natural mode oscillating at its natural frequency is referred to as a free oscillation of the scattering body. Notice that the free oscillations are completely independent of any excitation - they are characteristic of the scattering body itself. Finding the free oscillations is the first step toward solving the transient scattering problem via the SEM [4].

After its inception the SEM was applied to several simple perfectly conducting geometries. For examples, Tesche [16] considered the finite length thin wire, and Marin [7] considered the ϕ-independent electric type free oscillations of the prolate spheroid for various axial ratios. Over the years many geometries of increasing complexity have been analyzed.

After some experience was gained it became clear that the "possible entire function" is related to the early-time response before the scattering body is completely illuminated by the incident field. Morgan [13] suggests that it is only after the incident field is past the scattering body (late-time) that the scattered fields will be produced by the current associated with the free oscillations of the body. Before this time (early-time) the "driven" response contains, among other terms, a physical optics term. Heyman and Felsen [14], on the other hand, look at the early-time from the point of view of the geometrical theory of diffraction (GTD), which they merge with a constant coefficient sum of free oscillations in the late-time. The point is that the early-time response is highly dependent on the form of the incident excitation field (direction, polarization, time dependence), whereas the late-time response can be represented as a constant coefficient sum of free oscillations. Although the coefficients in this sum are incident field dependent, as determined via SEM, the free oscillations themselves are not. This is one of the beauties of the SEM. In particular, at any point in space, the scattering response in the late-time is a sum of exponentially damped sinusoids corresponding to the set of natural frequencies, which are unique to the particular scattering body. These natural frequencies can be extracted from a given scattering response via Prony's method [17], for example, and then used to identify the scattering body (with obvious applications in radar target identification [9], remote sensing, et cetera).

It should be mentioned, however, that most of the energy is contained in the early-time scattering response, especially for metallic scattering bodies with low-Q free oscillations (large surface area to volume ratios promoting rapid radiation damping) [13]. For instance, this results in practical difficulties in implementing some target identification schemes due to the low signal to noise ratio (SNR) of the late-time response [24]. However, there is progress being made in this area. For example, Chen *et al* [19] have proposed a new technique they call the 'radar waveform synthesis method', whereby the waveform of the incident radar pulse is chosen to excite the target in such a way that the late-time response contains only a single natural frequency. The principle application is in sensitively discriminating the *wrong* target. The advantage is that all of the return signal energy is concentrated in one free oscillation instead of being spread over many. Furthermore, this generally reduces the bandwidth (and hence noise energy, with appropriate filtering) of the returned signal.

Alternatively, consider periodically exciting the scattering body with a broad-band pulse, and then arithmetically averaging the responses over a large number of periods to virtually eliminate the noise (assuming the noise has zero mean) and thus recover the weak late-time response. Van Blaricum *et al* [23] point out that the standard deviation of the noise decreases as inverse square root of the number of trials run. This may be useful for identification of a stationary object buried in a homogeneous medium, for example. Or if the noise is due to "stray" responses of background objects (assumed fixed) on a radar range, for example, perhaps a catalog of this noise can be made in the absence of any intended target, and then later subtracted from the scattering response of intended target plus background. Thus, the low SNR difficulties are not insurmountable, and so the practical usefulness of the late-time response, especially in scattering object identification for which it is ideally suited, is not really diminished.

From a more academic point of view, the early-time and the late-time responses are duals of each other, especially in the sense of "progressing wave/oscillatory wave" put forth by Heyman and Felsen [14], and so are equally important, in principle, to a complete understanding of electromagnetic scattering phenomena.

The advantages of the SEM (for late-time response) over other techniques for solving transient or broad-band electromagnetic problems are well documented in the literature. Tesche [16] points out that more traditional methods like time harmonic analysis followed by Fourier inversion, or direct time domain solution depend on the incident field at an early stage; changing the incident field parameters means a considerable part of the solution must be recalculated. With the SEM, on the other hand, the bulk of the work involves determining the free oscillations and so called coupling vectors. Then each natural mode has a fixed coupling vector which, when combined with the incident field data, yields the coupling, or excitation coefficient for that particular free oscillation [4]. Thus changes in incident field parameters only affect the last stage of calculation. In [18] Baum compares several different techniques for transient or broad-band analysis. In particular, he stresses how rich the SEM is in terms of providing physical insight into the problem.

It is for all of the aforementioned reasons that we developed an interest in the analysis of the late-time response of scattering bodies using the SEM. As already mentioned the SEM has been applied to numerous single-body geometries. The first application to a two-body geometry was by Umashankar *et al* [10], who considered the finite length thin wire parallel to a ground plane (or wire and its image, with illumination antisymmetric with respect to the symmetry plane). They numerically generated the natural frequencies over a range of several parameters, but pointed to the difficulty in interpreting them, and the need for an analytical investigation. A follow-

up paper was published by Shumpert *et al* [11], which was similar, but allowed for circumferential variation of the axial current. Riggs *et al* [20] also considered the same problem, but varied the conductivity and permittivity of the ground plane. Crow *et al* [21] considered perpendicular crossed wires over a perfectly conducting ground plane. All of these provide limited physical interpretation; we could not find an analytical treatment of the two-body problem.

We should mention, though, that Riley *et al* [22] present a general theory combining the SEM with the classical theory of wave propagation in a multiple scattering environment. Then first derive (via the SEM) an expression for the far field transient response of a single scattering body to plane wave excitation, and then generalize to the case of multiple scattering bodies (in the far field of each other) by including not only the zero order terms (no interaction amongst the scatterers), but also a few higher order multiple scattering terms. They apply the theory in a statistical form to a random distribution of scatterers. This type of analysis is related to one suggested earlier by Umashankar *et al* [10]: "... one might prefer to treat a two-body problem in the time domain as a multiple-scattering problem between two single-body scatterers that have been individually characterized by the singularity expansion method." The point is that these schemes are really early-time analyses, and highly dependent on the incident field parameters; they do not consider the free oscillations (global resonances) of the multiple-body geometry as a whole, which apply in the late-time, and are the subject of interest in this present investigation.

Clearly, two perfectly conducting spheres is one of the simplest two-finite-body problems. An important source of difficulty, though, is that the wave equation does not separate in the bispherical coordinate system (or in any other two-finite-body coordinate system). Thus we must resort to the well known translational addition theorem

for representing one vector spherical wave function in one coordinate system in terms of those belonging to a translated coordinate system. Bruning and Lo [3] use such a scheme to solve the problem of time harmonic scattering from two spheres. Their derivation leads to a set of coupled infinite dimensional matrix equations of the form $Ax = b$, which they solve for the unknown x, in principle, by inverting the system matrix A and multiplying it into the right hand side source column matrix b. In chapter 2 we derive the corresponding homogeneous form $Ax = 0$ from the source free field equations, the solutions of which yield the free oscillations, and are the subject of the remainder of the thesis. In principle, the natural frequencies occur when the system determinant vanishes, and the corresponding null space is the natural mode(s) associated with that natural frequency.

Thus the basis goals of the thesis are to determine the free oscillations of two conducting spheres, for late-time applications as discussed above, and to discover properties of free oscillations unique to two (or more)-body geometries. Also, a two-body geometry presents the unique opportunity to treat each body as a local part of a single "distributed body" to examine in detail the mutual feedback, or coupling mechanisms that exist between the parts of a single body to sustain the free oscillation (except for radiation damping) without sources. The separation of the bodies places special emphasis on causality considerations. The fact that an analytical solution can be determined only for large sphere separation does not seriously limit these goals because most of the knowledge gained, by its very nature applies qualitatively to two spheres with any separation.

Because the geometry is invariant under rotation in ϕ the equations for different azimuthal number m are not coupled. In chapter 3 we obtain the solution to the $|m| = 1$ equations for large sphere separation d. First we find the zero order (in

$1/d$) translation coefficients (section 3.1). By a clever argument we circumvent calculation of the system matrix determinant, and yet obtain a transcendental equation for the natural frequencies (section 3.2). We analyze the properties of this equation in the complex frequency plane and numerically determine the natural frequencies in the limit $d \to \infty$. Let the sphere radii be a and b: We consider all cases $a = b$, $a \neq b$, and $b = 0$, and interpret the results (section 3.3). Then we determine and discuss the corresponding natural modes, for example symmetry considerations in the case $a = b$. In all cases we examine the interaction, or feedback fields that sustain a free oscillation, which provides a very interesting explanation of the logic behind the natural frequencies in terms of the dynamics of single-sphere scattering (section 3.4). Finally, we add first order (in $1/d$) correction terms to allow finite d, and determine what new information this provides (section 3.5).

Chapters 4 and 5 have a format similar to chapter 3, but consider cases $|m| \geq 1$ and $m = 0$, respectively. All calculations are done to first order in $1/d$. The emphasis is on the differences with the (now familiar) $|m| = 1$ case. Although for $|m| > 1$ the equation structure is only slightly modified, the details of the natural frequencies and natural modes are of course different. For $m = 0$ the equation structure is radically different, for now the electric and magnetic multipoles decouple (no longer hybrid natural modes). These differences are also reflected in the natural frequencies.

In chapter 6 we collect together the results of chapters 3 to 5 and present a discussion with conclusions, which contains a wealth of physical interpretation and insight into the problem. Most importantly we present a theory which links (most of) the two-sphere natural frequencies and natural modes with those of the single-sphere, introducing mechanisms apparently unique to multi-body geometries.

CHAPTER 2: FORMULATION OF THE PROBLEM

Consider two perfectly conducting spheres of radii a and b, separated by a distance d, embedded in a homogeneous, linear, and isotropic space, wherein the speed of propagation of an electromagnetic disturbance is c. We are interested in the electromagnetic fields which can exist in the presence of the spheres after all external sources of excitation have ceased. Such fields are called free oscillations, or natural modes [4]. It is well known (see, e.g., Stratton [1]) that, for the single sphere, free oscillations exist with a time dependence e^{st}, $s = \Omega + i\omega$, that is, an exponentially damped ($\Omega < 0$) sinusoid of frequency ω. We hypothesize that the same is true for the two sphere problem even if the spheres differ in radius. Thus we seek solenoidal solutions to the homogeneous vector wave equation (suppressed time dependence e^{st})

$$(\nabla \times \nabla \times - k^2)\, \mathbf{E}(\mathbf{r}) = 0, \qquad s = ikc, \tag{2.1}$$

subject to the boundary condition that the tangential components of the total electric field vanish on the surface of both spheres.

Following Stratton [1] we construct two linearly independent solenoidal vector solutions to (2.1), namely

$$\left.\begin{aligned} \mathbf{M} &= \nabla \times (\mathbf{r}\psi) = \frac{1}{k}\, \nabla \times \mathbf{N} \\ \mathbf{N} &= \frac{1}{k}\, \nabla \times \mathbf{M} \end{aligned}\right\} \tag{2.2}$$

where $(\nabla^2 + k^2)\psi = 0$, which in a spherical coordinate system (r,θ,ϕ) are the familiar magnetic and electric multipole fields:

$$\left.\begin{aligned}
\mathbf{M}_{lm}^{(j)}(k;r,\theta,\phi) &= z_l^{(j)}(kr)\, e^{im\phi} \left(\hat{\theta}\, \frac{im}{\sin\theta}\, P_l^m(\cos\theta) - \hat{\phi}\, \partial_\theta P_l^m(\cos\theta) \right) \\
\mathbf{N}_{lm}^{(j)}(k;r,\theta,\phi) &= \hat{r}\, \frac{1}{kr} z_l^{(j)}(kr)\, e^{im\phi}\, l(l+1)\, P_l^m(\cos\theta) \\
&\quad + \frac{1}{kr}\, \partial_r [r\, z_l^{(j)}(kr)]\, e^{im\phi} \left(\hat{\theta}\, \partial_\theta P_l^m(\cos\theta) + \hat{\phi}\, \frac{im}{\sin\theta}\, P_l^m(\cos\theta) \right)
\end{aligned}\right\} \tag{2.3}$$

where $l = 1, 2, \cdots$; $m = -l, -l+1, \cdots, l$; and $z_l^{(j)} = j_l, n_l, h_l^{(1)}, h_l^{(2)}$ for $j = 1, 2, 3, 4$ respectively, are spherical Bessel, Neumann, and Hankel functions. Any solenoidal vector field (over unrestricted angular variables) can be expressed as a linear combination of the multipole fields of type $j = 3$ and 4. In our case we have no sources at infinity and homogeneous space (except for the spheres) so that only type $j = 4$ (outward traveling waves) is acceptable.

In the usual way (see, e.g., Bruning and Lo [2]) we now introduce two coordinate systems O and O' centered on the spheres A and B, respectively, and related by a translation d along the z-axis (see Fig. 1). We adopt the convention that a primed quantity is referred to the O' system, whereas its unprimed counterpart is referred to the O system. Thus, the appropriate general solution to (2.1) is

$$\mathbf{E} = \sum_{l=1}^{\infty} \sum_{m=-l}^{l} \left(A_{lm}^E \mathbf{N}_{lm}^{(4)} + A_{lm}^H \mathbf{M}_{lm}^{(4)} + B_{lm}^E \mathbf{N}'^{(4)}_{lm} + B_{lm}^H \mathbf{M}'^{(4)}_{lm} \right) \tag{2.4}$$

Invoking the boundary conditions will generate a set of simultaneous equations for the unknown coefficients (the A's and B's).

To facilitate the application of the boundary conditions we need to be able to express primed quantities in terms of unprimed quantities and vice versa. For example, $\mathbf{M}'^{(4)}_{lm}$ is an outward traveling wave originating at O'; in the region $r < d$, which includes origin O, it must be expressible in terms of a linear combination of $\mathbf{M}_{\nu\mu}^{(1)}$ and

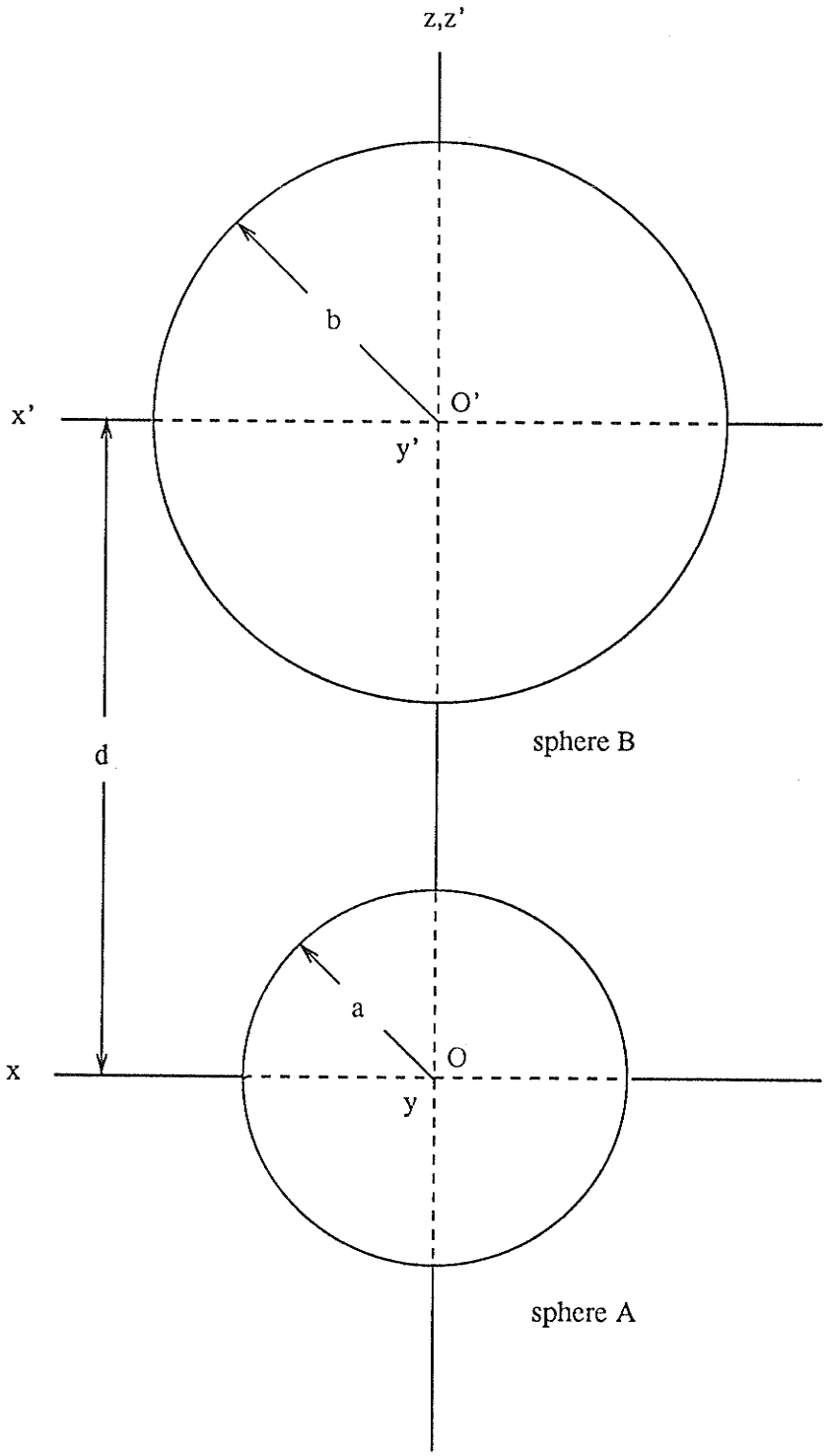

Fig 1: Geometry of two sphere problem

$\mathbf{N}^{(1)}_{\nu\mu}$. Since $\phi = \phi'$ only terms with $\mu = m$ will appear in the sum. Thus we construct the translation formula [2]

$$\mathbf{M}'^{(4)}_{lm} = \sum_{\nu=max(1,\,|\,m\,|\,)}^{\infty} \left[\alpha^{lm}_{\nu m}\mathbf{M}^{(1)}_{\nu m} + \beta^{lm}_{\nu m}\mathbf{N}^{(1)}_{\nu m} \right], \qquad r < d. \tag{2.5a}$$

Applying the curl operator to both sides immediately yields [see (2.2)]

$$\mathbf{N}'^{(4)}_{lm} = \sum_{\nu=max(1,\,|\,m\,|\,)}^{\infty} \left[\alpha^{lm}_{\nu m}\mathbf{N}^{(1)}_{\nu m} + \beta^{lm}_{\nu m}\mathbf{M}^{(1)}_{\nu m} \right], \qquad r < d \tag{2.5b}$$

where the α's and β's are called translation coefficients. For translating from the unprimed to the primed coordinate system we simply exchange primed and unprimed quantities in (2.5). Bruning and Lo [3] were apparently the first to note that (the parity of the Legendre functions implies)

$$\left.\begin{aligned} \alpha'^{lm}_{\nu m} &= (-1)^{\nu-l}\ \alpha^{lm}_{\nu m} \\ \beta'^{lm}_{\nu m} &= -\ (-1)^{\nu-l}\ \beta^{lm}_{\nu m} \end{aligned}\right\} \tag{2.6}$$

Hence, for $r < d$ we may write (2.4) as

$$\begin{aligned} \mathbf{E} = \sum_{l=1}^{\infty}\sum_{m=-l}^{l} \Bigg[& A^{E}_{lm}\mathbf{N}^{(4)}_{lm} + A^{H}_{lm}\mathbf{M}^{(4)}_{lm} \\ & + B^{E}_{lm} \sum_{\nu} \left[\alpha^{lm}_{\nu m}\mathbf{N}^{(1)}_{\nu m} + \beta^{lm}_{\nu m}\mathbf{M}^{(1)}_{\nu m} \right] \\ & + B^{H}_{lm} \sum_{\nu} \left[\alpha^{lm}_{\nu m}\mathbf{M}^{(1)}_{\nu m} + \beta^{lm}_{\nu m}\mathbf{N}^{(1)}_{\nu m} \right] \Bigg], \end{aligned} \tag{2.7}$$

or its counterpart in the primed coordinate system. Finally, applying the boundary conditions and using the orthogonality relations amongst the **M** and **N** vector functions over the θ, ϕ space, we arrive at the four coupled homogeneous equations:

$$
\left.
\begin{aligned}
\Lambda_l^E(ka)\, A_{lm}^E &= \sum_{\nu} \left[\alpha_{lm}^{\nu m} B_{\nu m}^E + \beta_{lm}^{\nu m} B_{\nu m}^H \right] \\
\Lambda_l^H(ka)\, A_{lm}^H &= \sum_{\nu} \left[\beta_{lm}^{\nu m} B_{\nu m}^E + \alpha_{lm}^{\nu m} B_{\nu m}^H \right] \\
\Lambda_l^E(kb)\, B_{lm}^E &= \sum_{\nu} \left[\alpha'^{\nu m}_{lm} A_{\nu m}^E + \beta'^{\nu m}_{lm} A_{\nu m}^H \right] \\
\Lambda_l^H(kb)\, B_{lm}^H &= \sum_{\nu} \left[\beta'^{\nu m}_{lm} A_{\nu m}^E + \alpha'^{\nu m}_{lm} A_{\nu m}^H \right]
\end{aligned}
\right\} \tag{2.8}
$$

where

$$
\Lambda_l^E(kr) = -\frac{\partial_r \left[r h_l^{(2)}(kr) \right]}{\partial_r \left[r j_l(kr) \right]}, \qquad \Lambda_l^H(kr) = -\frac{h_l^{(2)}(kr)}{j_l(kr)}
$$

$m = 0, \pm 1, \pm 2, \cdots$

$l, \nu \geq max(1, |m|)$

Notice that there is no coupling between multipole fields of different azimuthal number m so we have an independent set of equations for each value of m. The problem is to find the natural frequencies $s = ikc$ for which (2.8) admits solutions (the system determinant vanishes), and for each such s find the corresponding set of A and B coefficients (the system null space), which carries all information about the natural mode through (2.4). In case of degeneracy more than one natural mode will share the same natural frequency. Unfortunately it is not possible to obtain an exact solution. Instead we develop solutions valid for large sphere separation, with the hope that, in the process, we can still discover the salient features of the coupling mechanism.

CHAPTER 3: BASIC PRINCIPLES OF THE SOLUTION

Let us first make some reasonable conjectures about the coupling mechanism. Suppose that the field around sphere A (excluding the field incident from sphere B) is oscillating in a superposition of multipole fields (all with the same azimuthal number m and time dependence e^{st}). Similarly for sphere B. These fields are responsible for energy incident on their respective opposite spheres, which in turn couples to, or is the source of excitation for, the original set of multipole fields. In a sense we have mutually self-sustaining (but exponentially damped due to radiation) oscillations consistent, of course, with causality and the boundary conditions.

The transverse (to r) components of the multipole fields vanish on the z-axis except in the case $|m| = 1$ [see (2.3) and the Appendix]. Thus, we might expect that the coupling, as described above, would be strongest in this case, especially for large sphere separation. For example, two parallel dipoles will couple more strongly than two coaxial dipoles. Although we shall see that this understanding is incomplete, particularly in view of causality considerations, it turns out best to consider the $|m| = 1$ case first, if only for pedagogical reasons.

3.1 Translation Coefficients to Zero Order Approximation

To determine the translation coefficients in (2.5) we first need expressions for $\mathrm{M}'^{(4)}_{l,\pm1}$ and $\mathrm{N}'^{(4)}_{l,\pm1}$ in terms of the unprimed coordinates, valid at least in the neighborhood of sphere A ($r' \approx d$, $\theta' \approx \pi$, $\phi' = \phi$). The reason for requiring *both* the electric and magnetic multipoles will become apparent shortly.

To fix ideas we first consider a zero order approximation, which means that in all our calculations we neglect terms of order $1/kd$ or less with respect to terms of order unity. We demonstrate later that the resulting solution is the correct solution in the limit as the sphere separation $d \to \infty$. Without loss of generality we suppose that the sphere radii a and b are of order unity or less. Then, in the vicinity of sphere A, and to this order of approximation, we can write

$$\mathbf{M}'^{(4)}_{l,\pm 1} = \pm i^{-l+1}\, l(l+1)\, W_1\, e^{ikz}(\hat{x} \pm i\hat{y}) \tag{3.1}$$

$$\text{where } W_1 = \frac{i}{2}\,\frac{e^{-ikd}}{kd}, \text{ and}$$

$$\mathbf{N}'^{(4)}_{l,\pm 1} = \pm \mathbf{M}'^{(4)}_{l,\pm 1} \tag{3.2}$$

[see (2.3) and the Appendix]. In view of (2.5) and the orthogonality properties of the multipole fields, this latter result implies, to this order of approximation,

$$\beta^{l,\pm 1}_{\nu,\pm 1} = \pm \alpha^{l,\pm 1}_{\nu,\pm 1} \tag{3.3}$$

This relation represents an important simplification; we shall see this especially in the next section.

The circularly polarized uniform plane wave $e^{ikz}(\hat{x} \pm i\hat{y})$ is a solenoidal solution to the homogeneous vector wave equation (2.1), and so must be expressible in the form

$$e^{ikz}(\hat{x} \pm i\hat{y}) = (\hat{r}\sin\theta + \hat{\theta}\cos\theta \pm i\hat{\phi})\, e^{\pm i\phi} e^{ikr\cos\theta} \tag{3.4}$$

$$= \sum_{\nu=1}^{\infty} C_\nu^{\pm} \left[\, \mathbf{M}^{(1)}_{\nu,\pm 1} \pm \mathbf{N}^{(1)}_{\nu,\pm 1} \,\right]$$

where

$$\alpha^{l,\pm 1}_{\nu,\pm 1} = \pm i^{-l+1} l(l+1)\, W_1\, C_\nu^{\pm} \tag{3.5}$$

[see (3.1)] and we have made use of (3.3). Once we determine $C_\nu^{\pm}$ we have all the

translation coefficients by virtue of (3.5), (3.3), and (2.6). To this end we scalarly multiply both sides of (3.4) by $e^{-i\phi\hat{r}}$, and making use of (2.3) and the well known expansion

$$e^{ikr\cos\theta} = \sum_{\nu=0}^{\infty} i^{\nu}(2\nu + 1)\, j_{\nu}(kr)\, P_{\nu}(\cos\theta), \tag{3.6}$$

we have

$$\sum_{\nu=0}^{\infty} i^{\nu}(2\nu + 1)\, j_{\nu}(kr)\, \sin\theta\, P_{\nu}(\cos\theta) = \pm \sum_{\nu=1}^{\infty} C_{\nu}^{\pm}\, \frac{1}{kr}\, j_{\nu}(kr)\, \nu(\nu + 1)\, P_{\nu}^{1}(\cos\theta) \tag{3.7}$$

Applying some recurrence relations for the Legendre and spherical Bessel functions we finally have

$$C_{\nu}^{\pm} = \pm i^{\nu-1} \frac{(2\nu + 1)}{\nu(\nu + 1)}. \tag{3.8}$$

In summary, for $m = \pm 1$:

$$\left.\begin{aligned} \alpha_{lm}^{\nu m} &= i^{l-\nu} \frac{(2l + 1)}{l(l + 1)}\, \nu(\nu + 1)\, W_1(kd) \\ \beta_{lm}^{\nu m} &= \pm \alpha_{lm}^{\nu m} \\ \alpha'^{\nu m}_{lm} &= (-1)^{l-\nu} \alpha_{lm}^{\nu m} \\ \beta'^{\nu m}_{lm} &= -(-1)^{l-\nu} \beta_{lm}^{\nu m} \end{aligned}\right\} \tag{3.9}$$

where we have interchanged the indices l and ν for later convenience.

3.2 Solution of the Coupled Equations

First we will cast the coupled equations (2.8) into matrix form. We introduce new coefficients, which are simply the translation coefficients scaled by the factor W_1,

namely, for $m = \pm 1$,

$$\left.\begin{aligned} F_{lm}^{\nu m} &= \frac{\alpha_{lm}^{\nu m}}{W_1} = i^{l-\nu}\frac{(2l+1)}{l(l+1)}\nu(\nu+1) \\ G_{lm}^{\nu m} &= \frac{\beta_{lm}^{\nu m}}{W_1} = \pm F_{lm}^{\nu m} \\ F'^{\nu m}_{lm} &= \frac{\alpha'^{\nu m}_{lm}}{W_1} = (-1)^{l-\nu} F_{lm}^{\nu m} \\ G'^{\nu m}_{lm} &= \frac{\beta'^{\nu m}_{lm}}{W_1} = -+(1)^{l-\nu} F_{lm}^{\nu m} \end{aligned}\right\} \tag{3.10}$$

[see (3.9)]. (The double sign will always correspond to the cases $m = \pm 1$ unless otherwise noted). Now let us collect the $F_{lm}^{\nu m}$ coefficients into a matrix F, with row index l and column index ν. Similarly we form the matrices G, F', and G'. But (3.10) immediately implies

$$\left.\begin{aligned} G &= \pm F \\ F' &= JFJ \\ G' &= -+JFJ \end{aligned}\right\} \tag{3.11}$$

where J = diagonal[1, -1, 1, -1,...]. Notice that J commutes with any diagonal matrix and $J^2 = I$, the identity matrix. Finally, defining the matrix Λ = diagonal[Λ_n, Λ_{n+1},...], where $n = max(1, |m|) = 1$ in this case, and collecting the nonzero multipole coefficients into column matrices the coupled equations (2.8) become

$$\left.\begin{aligned} \Lambda^E(ka)\, A^E &= \quad W_1 F\ (B^E \pm B^H) \\ \Lambda^H(ka)\, A^H &= \pm W_1 F\ (B^E \pm B^H) \\ \Lambda^E(kb)\, B^E &= \quad W_1 JFJ\ (A^E -+ A^H) \\ \Lambda^H(kb)\, B^H &= -+W_1 JFJ\ (A^E -+ A^H) \end{aligned}\right\} \tag{3.12}$$

If the right hand side of these equations were zero then the first (second) pair of equations would describe an isolated sphere of radius a (b). For example, the electric type

natural modes for the single sphere (radius a) are the electric multipole fields; the set of natural frequencies are found from the roots of $\partial_a [a h_l^{(2)}(ka)] = 0$. All this is equivalent to the equation $\Lambda^E(ka)\, A^E = 0$.

The coupling structure of (3.12) is much simpler than that of the original (2.8); we owe this simplification to the approximations which led to (3.3). In particular, (3.12) immediately implies

$$\left.\begin{aligned} \Lambda^E(ka)\, A^E &= \pm\Lambda^H(ka)\, A^H \\ \Lambda^E(kb)\, B^E &= -+\Lambda^H(kb)\, B^H, \end{aligned}\right\} \tag{3.13}$$

which delineates the relative amplitudes of electric and magnetic multipole fields present in the natural mode (or modes) associated with frequency $s = ikc$; A_{lm}^E (B_{lm}^E) is directly proportional to A_{lm}^H (B_{lm}^H). Thus all natural modes of the two sphere geometry (at least for $|m| = 1$) are *hybrid* modes. Of course this is an obvious consequence of both electric and magnetic coefficients mixing on the right hand side of (3.12). We assume (and prove in the next section) that the natural frequencies never coincide with those of either sphere in isolation so that the Λ's can be inverted, which, since Λ is diagonal, is a trivial operation.

The right hand side of each equation in (3.12) is a column matrix, whose elements are exactly in the role of coefficients in a multipole expansion of an incident field, or excitation (from the opposite sphere). For example, in the first equation we call $W_1 F$ a *translation (matrix) operator*; it transforms the B coefficients (incident field) into a suitable set of excitation (or coupling) coefficients for sphere A. All of the geometry and frequency dependence of the translation operators is contained in the common scale factor

$$W_1 = \frac{i}{2}\frac{e^{-ikd}}{kd} \tag{3.14}$$

[see (3.1)]. In this sense W_1 is a measure of the strength of coupling, depending on sphere separation and frequency. We shall find that all natural frequencies correspond to k in the upper half k-plane. Thus we uncover the somewhat surprising fact that W_1 is dominated by an exponential *growth* as d becomes large! A little thought shows that this is a natural consequence of causality; we will understand its full significance in the next few sections.

Knowledge of any set of coefficients, say A^E, immediately implies the rest (A^H, B^E, and B^H) through (3.12). Thus we need only consider one set. Suitable substitutions, involving all four equations in (3.12), yields an equation containing only A^E, namely,

$$\left[I - [\Lambda^E(ka)]^{-1}\, D\, [\Lambda^E(ka)]\right] A^E = 0, \tag{3.15}$$

where we have defined

$$D = (W_1)^2\, F\, \Gamma(kb)\, F\, \Gamma(ka) \tag{3.16}$$

$$\Gamma(kr) = J\left[[\Lambda^E(kr)]^{-1} - [\Lambda^H(kr)]^{-1}\right] \tag{3.17a}$$

$$= \text{diagonal}[\Gamma_n(kr),\, \Gamma_{n+1}(kr),\ldots]$$

$$\Gamma_l(\zeta) = \frac{-i(-1)^{l-n}}{\zeta h_l^{(2)}(\zeta)\, \partial_\zeta[\zeta h_l^{(2)}(\zeta)]}, \tag{3.17b}$$

where, again, $n = max(1, |m|) = 1$ in this case. We have made use of a Wronskian relationship for spherical Bessel functions. Notice that the zeros of $\zeta h_l^{(2)}(\zeta)$ and $\partial_\zeta[\zeta h_l^{(2)}(\zeta)]$ determine the magnetic and electric natural frequencies for the isolated sphere, respectively. (Γ_l will play a significant role in determining the natural

frequencies).

Being homogeneous, (3.15) has solutions only for those natural frequencies $s = ikc$ which cause the determinant of the matrix in parentheses to vanish. An alternative to the quite formidable task of calculating the determinant is achieved by writing (3.15) as

$$A^E = [\Lambda^E(ka)]^{-1} D \; [\Lambda^E(ka)] A^E \tag{3.18}$$

which immediately implies

$$A^E = [\Lambda^E(ka)]^{-1} D^N \; [\Lambda^E(ka)] A^E \tag{3.19}$$

which must be true for any $N \in \{1, 2, ...\}$. We have shifted the work of calculating the determinant to calculating all powers of the matrix D. But this latter task is made almost trivial when we realize that F can be written in the form if an outer product of two column matrices U_m and V_m ($|m| = 1$), namely

$$F = U_m V_m^T, \quad \text{or} \quad F_{lm}^{\nu m} = U_{lm} V_{\nu m} \tag{3.20}$$

where

$$U_{l1} = i^l \frac{(2l+1)}{l(l+1)}, \quad V_{\nu 1} = i^{-\nu} \nu(\nu+1) \tag{3.21}$$

[see (3.10)]. Then, using (3.20) in (3.16) gives

$$D^N = \left[(W_1)^2 \chi_1(ka) \chi_1(kb) \right]^{N-1} D \tag{3.22}$$

where the scalar

$$\chi_1(kr) = V_1^T \Gamma(kr) U_1 = \sum_{l=1}^{\infty} U_{l1} V_{l1} \Gamma_l(kr). \tag{3.23}$$

Clearly we must have

$$[W_1(kd)]^2\, \chi_1(ka)\, \chi_1(kb) = 1 \tag{3.24}$$

which is a transcendental equation that permits us to determine the allowed natural frequencies $s = ikc$. Notice that (3.24) is independent of which coefficient set we are solving for [see (3.15)], is symmetric in a and b, and is insensitive to the sign of m ($m = \pm 1$). This latter fact gives rise to a basic two-fold degeneracy: Every $m = +1$ natural mode has a linearly independent (in fact orthogonal) $m = -1$ counterpart, both sharing the same natural frequency. The study of (3.24) is the subject of the next section. In the section following that we solve for the multipole coefficients (and hence the natural modes).

3.3 Natural Frequencies

We now discuss some properties of the function χ_1. Combining (3.23), (3.21), and (3.17b) we have

$$\chi_1(\zeta) = i \sum_{l=1}^{\infty} (-1)^l (2l + 1)\, \frac{1}{\zeta h_l^{(2)}(\zeta)\, \partial_\zeta [\zeta h_l^{(2)}(\zeta)]}. \tag{3.25}$$

The l^{th} term in the series ($l = 1, 2, 3, \ldots$) is an analytic function of ζ everywhere in the finite ζ-plane except at the zeros of $h_l^{(2)}(\zeta)$ and $\partial_\zeta[\zeta h_l^{(2)}(\zeta)]$, where it has poles. For any finite ζ, and $l \to \infty$ we can use the asymptotic formula

$$h_l^{(2)}(\zeta) \approx i\sqrt{2e}\, \frac{(2l + 1)^l}{(e\,\zeta)^{l+1}} \tag{3.26}$$

to show that the ratio of the $(l + 1)^{\text{th}}$ term to the l^{th} term of the series is of the order $(\zeta/2l)^2 \to 0$, and hence that the series is absolutely convergent for any finite ζ not at a pole of χ_1. Thus χ_1 is a meromorphic function. These poles of χ_1 correspond to the

electric and magnetic natural frequencies of a single isolated sphere and occur only in the upper half ζ-plane (left half s-plane).

As $\zeta \to 0$ the first term in the series dominates, and the limiting form for small argument is

$$\chi_1(\zeta) \approx -i\,3\zeta^3, \tag{3.27}$$

revealing a third order zero at the origin. A numerical investigation of (3.25) reveals only first order zeros, and only in the upper half ζ-plane, interspersed amongst the poles. These zeros will play an important role in our discussions. First notice that the zero at the origin is uniquely third order suggesting (correctly) that its physical significance is different from that of the other (first order) zeros.

χ_1 has no zeros or poles in the lower half ζ-plane. Except for some oscillatory behavior, $|\chi_1|$ essentially increases monotonically along any radial path from the origin into the lower half ζ-plane (or real ζ-axis).

Finally, we note that

$$h_l^{(2)}(-\zeta^*) = (-1)^l [h_l^{(2)}(\zeta)]^*, \tag{3.28}$$

where the asterisk denotes complex conjugation, implies the following parity property:

$$\chi_1(-\zeta^*) = [\chi_1(\zeta)]^*. \tag{3.29}$$

That is, the real part of χ_1 is symmetric and the imaginary part antisymmetric with respect to a reflection in the real ζ-axis. In particular, the magnitude of χ_1, and its zeros and poles are symmetrically disposed about the imaginary ζ-axis.

Of course we are still operating under the assumption that our results are correct only in the limit as the sphere separation $d \to \infty$. It is in this spirit that we now examine the transcendental equation (3.24). For k in the lower half complex plane

$[W_1(kd)]^2 \to 0$, so that for a solution to exist we need $\chi_1(ka)\chi_1(kb) \to \infty$ such that the product is unity. But $\chi_1(\zeta)$ is finite everywhere in the lower finite ζ-plane. Thus no modes of oscillation exist for k in the lower half plane (or natural frequency $s = ikc$ in the right half plane). This fact is, of course, easy to understand on physical grounds. With the time dependence e^{st} such a natural frequency would result in the fields (and thus the energy density at any given point) growing exponentially with the time, which is clearly unphysical since, by hypothesis, we have no sources at infinity, and we also consider the march of time only in the forward direction.

For k real and nonvanishing $[W_1(kd)]^2 \to 0$ again, but this time only as $1/(kd)^2$ since the exponential is of unit magnitude. Again (3.24) admits no solutions. Natural frequencies with $\Omega = 0$ (no damping) are reserved for interior (lossless cavity) modes; experience has shown that any time varying exterior mode must decay due to radiation. An exception to this rule can occur in the case of a perfect *dielectric* body. (see, for example, Stratton [1] section 9.23).

Let $k \to 0$ (and $d \to \infty$ as usual, but such that $kd \to 0$). Using (3.27) the limiting form of the left hand side of (3.24) is $\frac{9}{4}\frac{a^3b^3}{d^6}(kd)^4 \to 0$. Thus (3.24) cannot be satisfied for $k = 0$. This does not mean that no static (electric or magnetic) natural modes exist, it is simply a manifestation of the tacit assumption $k \neq 0$ that we used when setting up the original equations in chapter 2. The equation structure is different in the static cases, necessitating a separate treatment. In the electrostatic case, for example, instead of (2.1) we would write $\nabla \times \mathbf{E} = 0$ and $\nabla \cdot \mathbf{E} = 0$ outside the spheres. Then $\mathbf{E}$ can be derived from the gradient of a scalar potential satisfying the Laplace equation, et cetera. Then a treatment similar to that followed here could be used, or the fact that Laplace's equation is separable in the bi-spherical coordinate system provides an alternative solution path. Here we shall be concerned only with

time varying free oscillations. For some discussion about static natural modes in general see appendix A of Baum [5].

This leaves only the upper half k-plane, wherein $[W_1(kd)]^2 \to \infty$ so that $\chi_1(ka)\chi_1(kb)$ must vanish such that the product is unity. To fix ideas consider first the case of two identical spheres $a = b$. Equation (3.24) becomes

$$W_1(kd)\,\chi_1(ka) = \pm 1, \tag{3.30}$$

which suggests that we have two sets of solutions: one corresponding to the upper sign and the other to the lower sign (not to be confused with the cases $m = \pm 1$). Since the problem has a symmetry plane it must possess solutions (the fields or natural modes) of definite parity: symmetric and/or antisymmetric with respect to reflection in this plane. We shall see when we solve for the natural modes that the double sign in (3.30) *is* in fact the mark of parity. But when $d \to \infty$

$$\chi_1(ka) = \pm\frac{1}{W_1(kd)} \to 0 \tag{3.31}$$

so that the two sets of natural frequencies must coalesce in this limit (but of course the definite parity of the natural modes is invariant). In this case we have a four-fold degeneracy: two for $m = \pm 1$ times two for parity.

The solutions of (3.31) correspond to the natural frequencies s in the left half plane so that the free oscillations decay exponentially with time, consistent with radiation. Furthermore, the Hankel functions appearing in the expansion (2.4) contain the factors $\frac{e^{-ikr}}{r}$ and $\frac{e^{-ikr'}}{r'}$, respectively, so that we have outward traveling partial waves (or multipoles) which, at any instant of time, have the usual $1/r$ decay (energy conservation), but are dominated by an exponential growth in amplitude with radial distance from the spheres. The exponential growth is of course a necessary consequence of

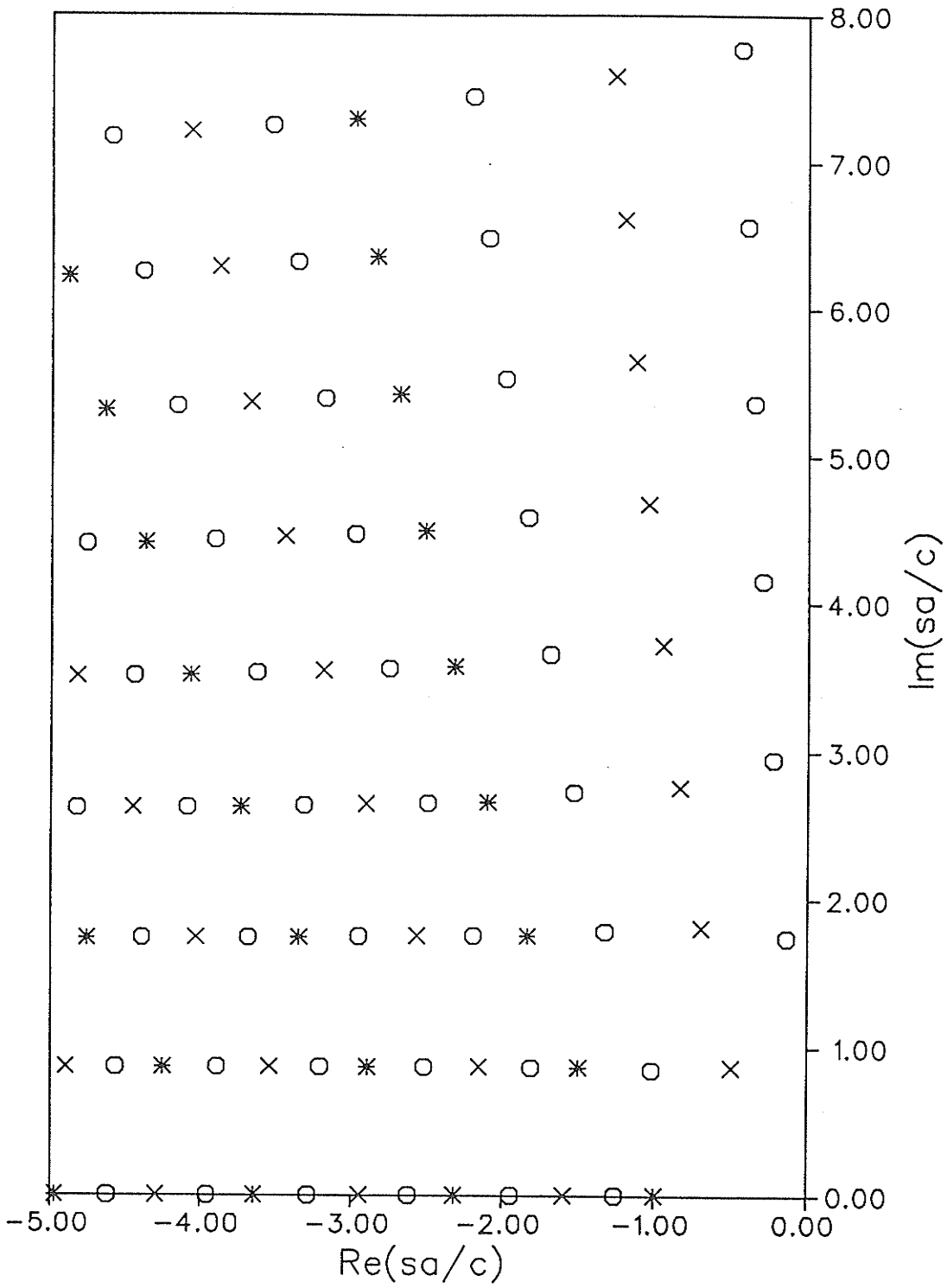

Fig 2: Natural frequencies for $d \to \infty$, $a=b$, $m=\pm 1$. For comparison the natural frequencies of a single sphere are indicated as $\times$(electric) and $*$(magnetic).

causality: the fields remote from the spheres are a measure of the fields near the spheres at an earlier time. Thus the "anomalous" factor W_1 appearing in the coupled equations (3.12). But we have yet to see in detail how nature allows infinite amplitude partial waves to be incident on their respective opposite spheres as $d \to \infty$.

We know that the zeros of $\chi_1(\zeta)$ are symmetrically disposed about the imaginary ζ-axis, which implies that the natural frequencies occur in complex conjugate pairs, as expected for any real system. In Fig. 2 we indicate the locations of the natural frequencies in the second quadrant of the normalized s-plane. Here

$$\frac{a}{c}\, s = ika = i\zeta \tag{3.32}$$

where ζ is a root of $\chi_1(\zeta) = 0$. Also shown for comparison is the set of natural frequencies (electric and magnetic type) for the single isolated sphere of radius a, where ζ is a root of $|\chi_1(\zeta)| = \infty$.

We first notice that the two sets are obviously distinct. This may be disturbing because our intuition may be saying: As the sphere separation increases the coupling should become less important until in the limit $d \to \infty$ the free oscillations reduce to those of two single spheres isolated by distance. Take for example the double harmonic oscillator studied in quantum mechanics: As the two potential wells separate, pairs of allowed energies coalesce until the energy spectrum reduces to that of a single isolated well. (see, for example, Merzbacher [6]). Or perhaps a closer analogy would be the mutual coupling that exists between any two elements of an antenna array, which becomes weaker between increasingly separated elements because the field decays primarily as the inverse of the distance (at sufficiently large element separation). But as discussed earlier, the free oscillations are exponentially damped in time causing the mutual coupling to be dominated by an exponential growth as sphere

separation d increases. The larger the sphere separation, the more important is the coupling, and so the results in Fig. 2 are not in conflict with intuition. For if the time dependence *did* correspond to a single sphere natural frequency then, just as in circuit theory, that single sphere natural mode (multipole) would resonate with infinite amplitude; the correct combination of multipoles could not exist to satisfy the necessary boundary conditions.

Let us study the results in Fig. 2 more closely. The natural frequencies tend to be grouped into so called "layers", typical of most geometries (see almost any literature on SEM, for example [4]). The first layer lies immediately to the left of, and almost parallel with the imaginary axis. To the left of this lies a layer of electric type natural frequencies for the single sphere, followed by the second layer of natural frequencies for the double sphere, and so on. The single sphere (electric and magnetic) layers are alternately "sandwiched" between the double sphere (hybrid) layers.

Natural frequencies in the first layer have the smallest magnitude of damping coefficient and hence resonate with the highest Q. The energy in these modes of oscillation is most tightly bound to the resonant structure (two spheres), even more so than is possible with a single sphere (with comparable size and frequency, namely the layer immediately to the left). A similar phenomenon occurs when a sphere is deformed into a prolate spheroid (keeping the major axis fixed), and finally into the thin rod limit (see Marin [7]), although the underlying physical mechanism is probably different. Notice that there are also natural frequencies on the real axis corresponding to an exponential decay in time, but no oscillation. Unfortunately we do not know how the natural frequencies move as a function of $d < \infty$, which might provide clues on how to further catagorize or label them.

We have been dealing with the special case $a = b$. Now let us go back to (3.24) and consider what happens when we set $b = 0$. Surely the presence of sphere B must vanish leaving only the single sphere A. As $kb \to 0$ (3.24) becomes, on using (3.27),

$$\chi_1(ka) \approx \frac{1}{-i\,3\,(kb)^3[W_1(kd)]^2}. \tag{3.33}$$

No matter how large we choose d [to ensure the correctness of (3.24)], when we set $b = 0$ the right hand side of (3.33) becomes infinite, thereby reducing (3.33) to the transcendental equation for the natural frequencies of a single isolated sphere of radius a, as expected. For example, suppose b to be infinitesimal such that the right hand side of (3.33) is large, and set $k = k_0 + \Delta k$, where $h_n^{(2)}(k_0 a) = 0$. This corresponds to a pure magnetic type free oscillation of the single sphere A, except perturbed infinitesimally by the presence of sphere B ($b \to 0$). Retaining only the largest term in the series expansion for $\chi_1(ka)$ (3.33) becomes

$$\frac{\Delta k}{k_0} \approx 3[W_1(kd)]^2 \frac{(-1)^n(2n+1)}{[h_n^{(2)\prime}(k_0 a)]^2} \left[\frac{b}{a}\right]^3 \tag{3.34}$$

provided $|\Delta k/k_0| \ll 1$; k reduces to k_0 when $b = 0$. The point of interest here is that the right hand side is proportional to the ratio of sphere *volumes*. Thus the physical significance of the *third* order zero of $\chi_1(\zeta)$ at the origin. (It is the machinery which handles the limiting case of one sphere vanishing).

Finally, we must discuss the case of nonvanishing unequal spheres ($a \neq b$). Imagine the exact solution when the sphere separation d is finite. When $a = b$ the natural modes have definite parity, either symmetric or antisymmetric, corresponding to different natural frequencies. As we make a different from b a symmetric mode will continuously deform into a new natural mode (no longer of definite parity), while the corresponding natural frequency will follow some smooth path in the s-plane to *its*

new value. Similarly for an antisymmetric natural oscillation. Now the words symmetric and antisymmetric have no physical meaning, but may be retained as labels to distinguish limiting behavior as $a \to b$.

We now examine this deforming of natural modes and movement of natural frequencies, but in the limit $d \to \infty$. We already know from (3.31) that for equal spheres pairs of natural frequencies (symmetric and antisymmetric) coalesce in this limit. (As mentioned before, this degeneracy is probably lifted for d finite). For slightly unequal spheres let us be democratic and set

$$a = r_0 + \Delta r \qquad \text{and} \qquad b = r_0 - \Delta r \tag{3.35}$$

where $|\Delta r| \ll r_0$, and Δr may be positive or negative. Expanding $\chi_1(ka)$ and $\chi_1(kb)$ in a Taylor series about kr_0 we write

$$\left.\begin{aligned} \chi_1(ka) &= \chi_1 + (k\Delta r)\,\chi_1' + \frac{1}{2}(k\Delta r)^2\,\chi_1'' + \cdots \\ \chi_1(kb) &= \chi_1 - (k\Delta r)\,\chi_1' + \frac{1}{2}(k\Delta r)^2\,\chi_1'' - \cdots \end{aligned}\right\} \tag{3.36}$$

with a radius of convergence equal to the distance to the nearest pole. For brevity in notation we write χ_1 for $\chi_1(kr_0)$. Using (3.36) in (3.24) we get a quadratic equation for χ_1, namely

$$0 = \chi_1^2 + (k\Delta r)^2\,\chi_1''\,\chi_1 - \left[(W_1)^{-2} + (k\Delta r)^2\,\chi_1'^2 + O[(k\Delta r)^4]\right] \tag{3.37}$$

We assume (and have numerically verified) that χ_1' and χ_1'' are never much greater than unity in magnitude, nor ever zero in regions of interest here. The two roots of (3.37) are

$$\chi_1 = -\frac{1}{2}(k\Delta r)^2\,\chi_1'' \pm \left[(W_1)^{-2} + (k\Delta r)^2\,\chi_1'^2 + O[(k\Delta r)^4]\right]^{1/2}. \tag{3.38}$$

In the case of vanishingly small difference in sphere radii we assume $|k\Delta r| \ll |(W_1)^{-1}| \ll 1$. Neglecting terms of order $(k\Delta r)^2$ with respect to unity (3.38) becomes

$$\chi_1(kr_0) = \pm \frac{1}{W_1(kd)} \left[1 + \frac{1}{2}(k\Delta r)^2 [W_1(kd)]^2\right] \to 0 \qquad (3.39)$$

in the limit $d \to \infty$. When $\Delta r = 0$ we recover (3.31) for the case $a = b$. Thus we identify the double sign in (3.38) as the mark of parity. For the purpose of discussion we mention here that the upper sign is for symmetric modes and the lower sign is for antisymmetric modes (we prove this in the next section). When $\Delta r \neq 0$, the magnitude of the second term in the parentheses is still much less than unity, by hypothesis, and so (3.39) is the transcendental equation for the case $a = b$ with a small first order correction term. But as $d \to \infty$ the correction term remains small [and hence (3.39) remains valid] only if $\Delta r \to 0$. This is the first hint that the nature of the solution changes very rapidly with the slightest perturbation from $a = b$ (at least in the limit $d \to \infty$).

Now let $\Delta r \neq 0$ such that $1 \gg |k\Delta r| \gg |(W_1)^{-1}|$. In the limit $d \to \infty$ this means any *nonzero* $|k\Delta r| \ll 1$. Then to first order in $(k\Delta r)$ (3.38) becomes

$$\chi_1(kr_0) = \pm (k|\Delta r|)\chi_1' \left[1 - + \frac{1}{2}(k|\Delta r|)\frac{\chi_1''}{\chi_1'}\right]. \qquad (3.40)$$

We first remind ourselves that the double sign appearing here is the same as that in (3.39). Thus, in making $\Delta r \neq 0$ the natural frequency belonging to the symmetric (antisymmetric) natural mode changed from its value when $a = b$ to a new value satisfying the transcendental equation (3.40) with the upper (lower) sign. Thus each pair of natural frequencies splits, the parity degeneracy having been lifted. [Recall that this degeneracy had its origins in the double sign in (3.30)] The second point to notice is

that (3.40) [and (3.39)] are insensitive to the sign of Δr. A bit of thought shows that this is a necessary consequence of the fact that one sphere is not preferred over the other.

Clearly the solutions of (3.40) are in the neighborhood of some $k = k_0$, where $\chi_1(k_0 r_0) \equiv 0$, so let us set $k = k_0 + \Delta k$. Here k_0 corresponds to the natural frequency when $\Delta r = 0$ and $d \to \infty$ [see (3.39)]. Writing $\chi_1(kr_0)$ in a Taylor series about $k_0 r_0$, and retaining only terms to first order in small quantities, (3.40) becomes

$$\frac{\Delta k}{k_0} = \pm \frac{|\Delta r|}{r_0} . \tag{3.41}$$

For $\Delta r = 0$ we use (3.39), which tells us $\Delta k = 0$ (in the limit $d \to \infty$). For $|\Delta r| > 0$ (but much less than r_0) we use (3.41). Thus the parity degeneracy is lifted to first order in Δr. From (3.41) we make an interesting observation: As we make $\Delta r \neq 0$, the *symmetric* natural frequency *increases* in magnitude (higher frequency and more rapidly damped), while the *antisymmetric* one *decreases* by the same amount. Analogous phenomena happen, for example, in the case of two coupled classical harmonic oscillators.

As an alternative approach to the case $a \neq b$, let us start again at (3.24). For $a \neq b$ two solutions immediately present themselves:

$$\left.\begin{aligned} \chi_1(k_a a) &= \frac{1}{\chi_1(k_a b)\,[W_1(k_a d)]^2} \to 0, \quad \text{where} \quad \chi_1(k_a b) \neq 0, \quad \text{and} \\ \chi_1(k_b b) &= \frac{1}{\chi_1(k_b a)\,[W_1(k_b d)]^2} \to 0, \quad \text{where} \quad \chi_1(k_b a) \neq 0. \end{aligned}\right\} \tag{3.42}$$

We point out that these expressions approach zero like $(W_1)^{-2}$ instead of just $(W_1)^{-1}$ as $d \to \infty$. [see (3.31) for the case $a = b$]. This fact will become important to our understanding of how the natural modes work in the case $a \neq b$. Using (3.35) again,

but this time with no restriction on the size of Δr (except $0 < |\Delta r| < r_0$), and $\chi_1(k_0 r_0) \equiv 0$, we have

$$\left.\begin{aligned} k_a &= k_0 \frac{r_0}{a} \approx k_0 \left[1 - \frac{\Delta r}{r_0}\right], \quad \text{for} \quad \frac{|\Delta r|}{r_0} \ll 1 \\ k_b &= k_0 \frac{r_0}{b} \approx k_0 \left[1 + \frac{\Delta r}{r_0}\right], \quad \text{for} \quad \frac{|\Delta r|}{r_0} \ll 1. \end{aligned}\right\} \tag{3.43}$$

With $r_0 = a$ the set of natural frequencies corresponding to the k_a's are exactly those appearing in Fig. 2, while those corresponding to the k_b's are simply the same set, except scaled by the factor a/b. We can identify pairs in the limit $\Delta r \to 0$. In (3.43), for $|\Delta r|/r_0 \ll 1$, we identify the Δk appearing in (3.41). Furthermore, the smaller (larger) sphere is associated with a larger (smaller) magnitude of natural frequency and hence to the deformed symmetric (antisymmetric) natural mode. The exact meaning of "associated with" will become clear during our discussion of the natural modes.

3.4 Natural Modes

We now turn our attention to the expansion coefficients in (2.4), which are the essence of the natural modes themselves. As usual, the $\pm$ sign used throughout will refer to the cases $m = \pm 1$ unless otherwise noted. Writing (3.18) out in detail [using (3.16), (3.20), and (3.23)] we have, for the A^E set of expansion coefficients,

$$A^E = \left\{ [W_1(kd)]^2 \, \chi_1(kb) \, V^T \, \Gamma(ka) \, \Lambda^E(ka) \, A^E \right\} [\Lambda^E(ka)]^{-1} \, U_1. \tag{3.44}$$

The homogeneous nature of equations (2.8) allows us to set the scalar in braces to any convenient value, say unity. Then the remaining coefficients are fixed via (3.12),

namely

$$\left.\begin{aligned} A^E &= [\Lambda^E(ka)]^{-1}\, U_1 \\ A^H &= \pm[\Lambda^H(ka)]^{-1}\, U_1 \\ B^E &= W_1(kd)\, \chi_1(ka)\, [\Lambda^E(kb)]^{-1}\, JU_1 \\ B^H &= -\!\!+W_1(kd)\, \chi_1(ka)\, [\Lambda^H(kb)]^{-1}\, JU_1 \end{aligned}\right\}. \tag{3.45a}$$

Notice the asymmetry between the *form* of the A and B coefficient sets. The *dual form* can be obtained from (3.45a) simply by rescaling all the coefficients by the factor $W_1(kd)\, \chi_1(kb)$. On using (24) we have

$$\left.\begin{aligned} A^E &= W_1(kd)\, \chi_1(kb)\, [\Lambda^E(ka)]^{-1}\, U_1 \\ A^H &= \pm W_1(kd)\, \chi_1(kb)\, [\Lambda^H(ka)]^{-1}\, U_1 \\ B^E &= [\Lambda^E(kb)]^{-1}\, JU_1 \\ B^H &= -\!\!+[\Lambda^H(kb)]^{-1}\, JU_1, \end{aligned}\right\} \tag{3.45b}$$

which demonstrates the symmetry that must be present in the equation structure (one sphere is not preferred over the other). The "extra" J in the B set of coefficients and the $-\!\!+$ instead of $\pm$ have their origins in the fact that we simply *translated* the O' coordinate system (Fig. 1) instead of translating and inverting the z'-axis ($\theta' \rightarrow \pi - \theta'$). The latter set of operations produces a left handed coordinate system O', which is a mirror image of the O system in the plane $z = d/2$ or $z' = -d/2$. Either set (3.45a) or (3.45b) may be used, whichever is more convenient. (Actually, multiplying (3.45a) by $[W_1\, \chi_1(kb)]^{1/2}$ or (3.45b) by $[W_1\, \chi_1(ka)]^{1/2}$ results in a more symmetric form, but not suited for our discussion).

As a double check on the correctness of (3.45a or b) it is easy to demonstrate by direct substitution that the coefficients satisfy the original equations (3.12), provided the transcendental equation (3.24) is satisfied.

Let us examine the convergence of the natural mode partial wave expansion (2.4). For example, from (3.45a) the magnetic coefficients for sphere A are

$$A_{lm}^{H} = \pm \left[\Lambda_l^H(ka)\right]^{-1} U_{l1} = -+ i^l \frac{(2l+1)}{l(l+1)} \frac{j_l(ka)}{h_l^{(2)}(ka)} , \tag{3.46}$$

[see (3.21) and (2.8)]. Using formulas like (3.26) we can show that for any given finite ka, and $l \to \infty$

$$A_{lm}^{H} \approx \pm \frac{i^{l+1}}{2} \frac{(2l+1)}{l(l+1)} \left[\frac{eka}{2l+1}\right]^{2l+1} \to 0, \text{ and} \tag{3.47a}$$

$$\frac{A_{l+1,m}^{H}}{A_{lm}^{H}} \approx i \frac{l}{(l+2)} \left[\frac{2l+1}{2l+3}\right]^{2l} \left[\frac{eka}{2l+3}\right]^{2} \to 0 \tag{3.47b}$$

and similar expressions for the other coefficients. For the most part, the magnitude of the coefficients decreases with increasing l (at least for sufficiently large l). Without further ado, by inspection of (3.46) and (2.3) we state the self evident fact that (2.4) converges at all points in space.

It is interesting to observe from (3.47) that the larger $|k|$ is, the more terms are required for convergence of the sum (2.4). In other words, natural modes with larger *magnitude* of natural frequency have more higher order multipole field components, insensitive as to whether this magnitude is due primarily to ω (rapid oscillation with little damping) or to Ω (rapid damping with no oscillation), or a combination. The basic reason is that both result in a rapid spatial variation of the field.

Now take the special case $a = b$. We introduce the dichotomic parity variable p which can take on one of two values: +1 for even parity (symmetric) or -1 for odd parity (antisymmetric) natural modes. Using

$$W_1(kd)\, \chi_1(ka) \equiv p \tag{3.48}$$

[see (3.30)] in either (3.45a) or (3.45b) results in

$$\left.\begin{aligned} A^E &= [\Lambda^E(ka)]^{-1}\, U_1 \\ A^H &= \pm\, [\Lambda^H(ka)]^{-1}\, U_1 \\ B^E &= p\ [\Lambda^E(ka)]^{-1}\, JU_1 \\ B^H &= -+\, p\ [\Lambda^H(ka)]^{-1}\, JU_1. \end{aligned}\right\} \tag{3.49}$$

As mentioned earlier, had we inverted the z'-axis the A and B coefficient sets would be identical except for a possible overall sign difference, which here is represented by p. (Of course then we would also require two different definitions of the multipoles: one for right and one for left handed coordinate systems). As it stands,

$$\left.\begin{aligned} B^E_{lm} &= -p\ (-1)^l\ A^E_{lm} \\ B^H_{lm} &= p\ (-1)^l\ A^H_{lm}\ , \end{aligned}\right\} \tag{3.50}$$

the $-(-1)^l$ coming from the matrix J. This result, coupled with the fact that inversion of the z-axis, or $\theta \to \theta - \pi$, transforms $P_l^m(\cos\theta)$ into $(-1)^{l+m}\ P_l^m(\cos\theta)$, makes it intuitively plausible that p is in fact the mark of parity as we claim, but this still awaits a formal proof. But before we do so, let us digress a moment to briefly review symmetry in electromagnetics.

Suppose that an electric field $\mathbf{E}$ satisfies (2.1) and boundary conditions which are symmetric with respect to the $z = 0$ plane. Consider another field $\mathbf{E}'$ obtained from $\mathbf{E}$ by replacing z with $-z$ and $\hat{z}$ with $-\hat{z}$ (reflection in the $z = 0$ plane). By expanding the $\nabla \times \nabla \times$ operator in Cartesian coordinates it is easy to show that $\mathbf{E}'$ also satisfies the same differential equation (2.1). Since it also manifestly satisfies the boundary conditions, $\mathbf{E}'$ is another solution. Then, by linearity, so is $\mathbf{E} \pm \mathbf{E}'$, which has even parity (symmetric with respect to reflection in the $z = 0$ plane) or odd parity (antisymmetric), respectively. (i.e., solutions of definite parity exist). We also note that since

the magnetic field is proportional to the curl of the electric field we can show that the two must have opposite parity.

Thus we must prove that $\mathbf{E}$ in (2.4) (drop the sum over m) evaluated at the point r, θ, ϕ is equal to $p\mathbf{E}$ evaluated at the point $r' = r, \theta' = \pi - \theta, \phi' = \phi$ *with* $\hat{\ell}' \equiv -\hat{\ell}$. The first quantity is [see (2.7)]

$$\sum_{l=1}^{\infty} \Bigg[A_{lm}^{E}\mathbf{N}_{lm}^{(4)} + A_{lm}^{H}\mathbf{M}_{lm}^{(4)} - p\ (-1)^{l}\ A_{lm}^{E} \sum_{\nu} \left(\alpha_{\nu m}^{lm}\mathbf{N}_{\nu m}^{(1)} + \beta_{\nu m}^{lm}\mathbf{M}_{\nu m}^{(1)} \right) + p\ (-1)^{l}\ A_{lm}^{H} \sum_{\nu} \left(\alpha_{\nu m}^{lm}\mathbf{M}_{\nu m}^{(1)} + \beta_{\nu m}^{lm}\mathbf{N}_{\nu m}^{(1)} \right) \Bigg],$$

where we have made use of (3.50). The second quantity is

$$\sum_{l=1}^{\infty} \Bigg[-(-1)^{l}\ A_{lm}^{E}\mathbf{N}'^{(4)}_{lm} + (-1)^{l}\ A_{lm}^{H}\mathbf{M}'^{(4)}_{lm} + p\ (-1)^{l}\ A_{lm}^{E} \sum_{\nu} (-1)^{\nu} \left(\alpha_{\nu m}^{lm}\mathbf{N}'^{(1)}_{\nu m} - \beta_{\nu m}^{lm}\mathbf{M}'^{(1)}_{\nu m} \right) + p\ (-1)^{l}\ A_{lm}^{H} \sum_{\nu} (-1)^{\nu} \left(\alpha_{\nu m}^{lm}\mathbf{M}'^{(1)}_{\nu m} - \beta_{\nu m}^{lm}\mathbf{N}'^{(1)}_{\nu m} \right) \Bigg],$$

where we made use of (2.6), and it is understood that in the vector functions $r' = r, \theta' = \pi - \theta, \phi' = \phi$, and $\hat{\ell}' = -\hat{\ell}$. Inspection of (2.3) reveals that in this case $\mathbf{M}'^{(j)}_{lm} = (-1)^{l}\ \mathbf{M}^{(j)}_{lm}$, and since $\mathbf{N}$ is proportional to the curl of $\mathbf{M}$, $\mathbf{N}'^{(j)}_{lm} = -(-1)^{l}\ \mathbf{N}^{(j)}_{lm}$. Thus the two quantities are equal and the natural modes are symmetric or antisymmetric with respect to the $z = d/2$ plane according to whether p in (3.49) is +1 or -1. Strictly speaking this proof is valid only in a region which is the union of $r < d$ and $r' < d$. But this is sufficient to fix the symmetry nature of the currents on the spheres and thus of the field everywhere in space.

We have already discussed the basic coupling mechanism which is responsible for the existence of free oscillations in the two sphere geometry. The energy in the field oscillating about one sphere comes from energy incident from the other sphere and vice-versa, and all the while energy is being given up to radiation to infinity. The field incident from sphere B onto sphere A is

$$\mathbf{E}^{\text{inc}}_{B\to A} = \sum_{l=1}^{\infty} \left[B^E_{lm}\mathbf{N}'^{(4)}_{lm} + B^H_{lm}\mathbf{M}'^{(4)}_{lm} \right] \tag{3.51}$$

$$= \sum_{l=1}^{\infty}\sum_{\nu=1}^{\infty} \alpha^{\nu m}_{lm} \left(B^E_{\nu m} \pm B^H_{\nu m}\right) \left(\mathbf{N}^{(1)}_{lm} \pm \mathbf{M}^{(1)}_{lm}\right)$$

where we used the translation formulas and (3.3), and interchanged l and ν for convenience. But

$$\sum_{\nu=1}^{\infty} \alpha^{\nu m}_{lm} \left(B^E_{\nu m} \pm B^H_{\nu m}\right) = \left[W_1 F \left(B^E \pm B^H\right)\right]_l , \tag{3.52}$$

the l^{th} excitation coefficient for sphere A, as expected [see right hand side of (3.12)]. Starting with (3.49) we find that this coefficient is simply U_{l1} in (3.21). It is easy to establish the following identities:

$$\left.\begin{aligned} \left(\hat{x} \pm i\hat{y}\right) e^{ikz} &= -i \sum_{l=1}^{\infty} U_{l1} \left(\mathbf{N}^{(1)}_{lm} \pm \mathbf{M}^{(1)}_{lm}\right) \\ \left(\hat{x}' \pm i\hat{y}'\right) e^{-ikz'} &= +i \sum_{l=1}^{\infty} U^*_{l1} \left(\mathbf{N}'^{(1)}_{lm} - \mathbf{M}'^{(1)}_{lm}\right) , \end{aligned}\right\} \tag{3.53}$$

the first of which was derived in section 3.1. Using this in (3.51) we find that

$$\mathbf{E}^{\text{inc}}_{B\to A} = i \left(\hat{x} \pm i\hat{y}\right) e^{ikz} \tag{3.54}$$

is a right or left ($m = \pm 1$) circularly polarized uniform plane wave with magnitude of order unity. This is exactly the mode of interaction the energy transferred between the spheres would be expected to adopt: A plane wave because of the great distance d

between phase centers, circularly polarized because of the $e^{im\phi}$ factor in the multipoles, and of order unity because the coefficients A^E and A^H of the scattered field are also of order unity. But recall that the amplitudes of the individual partial waves making up the incident field (3.54) are of order $|W_1(kd)| \to \infty$ [see the individual terms in (3.51)]! The only conclusion is that there must be almost perfect destructive interference amongst the partial waves radiated from sphere B, at least in the neighborhood of sphere A.

Recall that the real part of ik is Ω/c, which is negative. Thus the incident field at any instant of time increases exponentially in the direction of propagation. The ratio of the amplitude at the farthest point on the shadow side ($z = -a$) to that on the corresponding point on the illuminated side ($z = a$) is $\exp\left[-\frac{2a}{c}\Omega\right]$. For the first natural frequency in the first layer (Fig. 2) this ratio is about 1.32, which is the smallest of all the modes. The corresponding wavelength is about $3.61a$. The next natural frequency with about the same wavelength is the second one in the second layer; its amplitude ratio is about 14.3 already! Thus even within the first few lowest order natural modes this ratio can be quite large.

We can thus describe the incident field at any instant of time along the axis joining sphere A to B: Starting at sphere B it has about unit magnitude. A short distance away the exponential growth in $W_1(kr)$ begins to dominate and the field continues to grow in magnitude until the zero order asymptotic form for the spherical Hankel function becomes a good approximation. Then destructive interference amongst the partial waves sets in, and finally dominates as we approach sphere A. The incident field is now a plane wave which, at any point decreases exponentially with time and so, at any time, must increase exponentially in the direction of propagation, going from almost

zero on the illuminated side ($z > 0$) to order unity at $z = 0$ and finally, rapidly to infinity on the shadow side ($z < 0$). Of course there is a similar wave traveling in the opposite direction from sphere A to B. We discuss the off-axis behavior of these fields when we consider first order corrections in the next section.

The incident field (3.54) scatters from sphere A. It can be shown that the coefficients in the multipole expansion of this scattered field are exactly just the A^E and A^H, as expected. This field then acts as $\mathbf{E}^{\text{inc}}_{A\to B}$, which is similar in form to the second of (3.53) in the neighborhood of sphere B, and so on. $\mathbf{E}^{\text{inc}}_{A\to B}$ is just the back scattered field to $\mathbf{E}^{\text{inc}}_{B\to A}$, and vice-versa. Thus the natural frequencies are just those (complex) frequencies at which a plane wave incident on a conducting sphere has almost a back scattering null (as $d \to \infty$). In fact, $|\chi(ka)|^2$ is proportional to the echo area of a conducting sphere of radius a which, according to (3.31) must vanish at the natural frequencies. (See Harrington [8] equation (6-105)). Harrington plots $\frac{\pi}{k^2}|\chi(ka)|^2$ in his Fig. 6-12 for real k; we examine its behavior for complex k in Fig. 2. In this new light, the poles correspond to the single sphere natural frequencies where an incident plane wave of that frequency would excite an infinite response, which implies an infinite echo area. The zeros on the other hand correspond to double sphere natural frequencies where an incident plane wave of that frequency has almost exactly a back scattering null (to compensate for causality considerations in signals that decay in time). This implies zero echo area.

We now examine the case $b = 0$. We already know that the natural frequencies reduce to those of the single sphere. Furthermore, inspection of (3.45a) reveals that only the one A_{lm} corresponding to that natural frequency becomes infinite, the rest remaining finite. A rescaling of all the coefficients then implies that the double sphere natural mode reduces to that unique single sphere multipole (natural mode); all other

multipoles have vanishing contribution. Incidentally, the B coefficients in (3.45a) also vanish. As $kb \to 0$, and with the above rescaling in mind,

$$\left.\begin{aligned} B^E_{lm} &\approx \frac{-(-i)^l}{3l^2\,[1\cdot3\cdot5\cdots(2l-1)]^2}\,\frac{(kb)^{2(l-1)}}{W_1(kd)} \to 0 \\ B^H_{lm} &\approx \frac{(-i)^l}{3l(l+1)\,[1\cdot3\cdot5\cdots(2l-1)]^2}\,\frac{(kb)^{2(l-1)}}{W_1(kd)} \to 0 \end{aligned}\right\} \tag{3.55}$$

for all $l = 1, 2,...$ This last result is just a further indicator of the self consistency of the solution.

Lastly, we examine the case $a \neq b$. Recall that the natural frequencies come in pairs s_a and s_b [corresponding to k_a and k_b; see (3.42) and (3.43)]. Let us first discuss the natural mode corresponding to s_a. Using the first of (3.42) in (3.45a) we have

$$\left.\begin{aligned} A^E &= [\Lambda^E(k_a a)]^{-1}\,U_1 \\ A^H &= \pm\,[\Lambda^H(k_a a)]^{-1}\,U_1 \\ B^E &= \frac{1}{W_1(k_a d)\,\chi_1(k_a b)}\,[\Lambda^E(k_a b)]^{-1}\,JU_1 \to 0 \\ B^H &= -+\,\frac{1}{W_1(k_a d)\,\chi_1(k_a b)}\,[\Lambda^H(k_a b)]^{-1}\,JU_1 \to 0. \end{aligned}\right\} \tag{3.56}$$

Thus the A coefficients are of order unity as before, but the B coefficients (and hence the currents on sphere B) vanish as $(W_1)^{-1}$, even if the sphere radii differ only infinitesimally! Our earlier suspicions about the rapid change in the nature of the oscillations when we perturb the relative sphere size have been realized.

We can understand how the natural mode "works" by examining the interaction fields between the spheres, just as we did for the case $a = b$. In fact, comparing (3.56) with (3.49) reveals that these fields are still circularly polarized uniform plane

waves, just the amplitudes have been changed. Making use of the first of (3.53) and the B coefficients in (3.56) we can show that

$$\mathbf{E}^{\text{inc}}_{B\to A} = i\ (\hat{x} \pm i\hat{y})\ e^{ikz}. \tag{3.57}$$

This plane wave of order unity magnitude strikes sphere A and is scattered. The induced currents and the A coefficients are of order unity like the incident field. On the other hand, making use of the second of (3.53) and the A coefficients in (3.56) we can show that

$$\mathbf{E}^{\text{inc}}_{A\to B} = \frac{1}{W_1(k_a d)\ \chi_1(k_a b)}\ i\ (\hat{x}' \pm i\hat{y}')\ e^{-ikz'} \ \to 0. \tag{3.58}$$

This plane wave of order $(W_1)^{-1} \to 0$ magnitude strikes sphere B and is scattered. The induced current and the B coefficients vanish as $d \to \infty$, like the incident field.

So how does the asymmetry of the natural mode arise? We first notice that by choosing $s = s_a$ sphere A is "matched" to the incident plane wave, that is, $\mathbf{E}^{\text{inc}}_{B\to A}$ striking sphere A has almost a back scattering null in the region of sphere B. The important point is that the destructive interference here is far more complete than it was in the case $a = b$. Here the back scattered field in the neighborhood of sphere B ($\mathbf{E}^{\text{inc}}_{A\to B}$) is of order $(W_1)^{-1} \to 0$, instead of order unity as it was in the case $a = b$. The better matching in the former case is directly related to the fact that the right hand side of (3.42) vanishes as $(W_1)^{-2}$ compared to only $(W_1)^{-1}$ in (3.31). If the right hand side were *identically* zero in either of these expressions, a plane wave of the corresponding frequency would have an *exact* back scattering null at infinity. Conversely, with $s = s_a$ sphere B is *not* matched to the incident plane wave ($\mathbf{E}^{\text{inc}}_{A\to B}$). The scattered field starts out with a magnitude of order $(W_1)^{-1}$. In the region of sphere A it must be a plane wave, similar in form to the first of (3.53), but the magnitude has been increased by a factor W_1 because now there is no (appreciable)

destructive interference amongst the partial waves. Thus $\mathbf{E}^{\text{inc}}_{B\to A}$ has a magnitude of order unity, as we see in (3.57). The asymmetry in the natural mode is thus explained.

The second solution follows from choosing $s = s_b$. Using the second of (3.42) in (3.45b) we have

$$\left.\begin{aligned} A^E &= \frac{1}{W_1(k_b d)\,\chi_1(k_b a)}\,[\Lambda^E(k_b a)]^{-1}\,U_1 \;\to 0 \\ A^H &= \pm\,\frac{1}{W_1(k_b d)\,\chi_1(k_b a)}\,[\Lambda^H(k_b a)]^{-1}\,U_1 \;\to 0 \\ B^E &= [\Lambda^E(k_b b)]^{-1}\,JU_1 \\ B^H &= -+\,[\Lambda^H(k_b b)]^{-1}\,JU_1. \end{aligned}\right\} \qquad (3.59)$$

This is the dual mode: The currents on sphere B are of order unity, while those on sphere A vanish as $(W_1)^{-1}$. It is now sphere B which is matched to the incident plane wave of frequency s_b, and sphere A is unmatched, et cetera.

Now suppose $a < b$. This implies $|\,s_a\,| > |\,s_b\,|$ [see (3.43)]. Thus the natural mode corresponding to $s = s_a$ (s_b) is the deformed symmetric (antisymmetric) mode. The converse is true if $b < a$. In other words, the mode associated with, or matched to, the smaller (larger) sphere is the deformed symmetric (antisymmetric) mode.

3.5 First Order Corrections

We now understand that the existence of free oscillations as $d\to\infty$ relies on almost perfect destructive interference between the partial waves (multipole fields) incident on each sphere from its respective opposite sphere. This raises a question as to the validity of our zero order approximation. In particular, in writing (3.1) we have

retained only the first term in the standard finite series representation of the spherical Hankel function, and throughout have neglected all terms of order $1/kd$ and higher with respect to unity. But the almost perfect destructive interference demands a delicate and precise relationship between the complex amplitudes of the partial waves. Perhaps using our approximations (3.1) and (3.2) in place of the exact expressions for the partial waves significantly changes the solution, leading us to doubt the results derived thus far, even in the limit $d \to \infty$. To alleviate such concerns we shall in this section, and in a condensed manner, repeat the material of sections 3.1 to 3.4, but this time retaining all terms to order $1/kd$, that is, correct to first order.

But before we begin the first order correction proper, let us carry out a simple double check which, although limited in scope, provides some useful insight. In the case $a = b$ the details of the destructive interference are embedded in the steps leading from (3.51) to (3.54). Let us repeat this calculation, but use the exact expressions for the multipoles instead of the approximations in (3.1) and (3.2). For simplicity we limit ourselves to finding $\mathbf{E}^{\text{inc}}_{B \to A}$ only at one point - the center of sphere A. The appropriate multipole fields are [see (2.3) with $r' = d$, $\theta' = \pi$, $\phi' = \phi$, $\hat{\theta}' = -\hat{\beta}$, $\hat{\phi}' = \hat{\phi}$]:

$$\left.\begin{aligned} \mathbf{M}'^{(4)}_{lm} &= \pm i\ (-1)^l\ l(l+1)\ \frac{1}{2}\ h_l^{(2)}(kd)\ (\hat{x} \pm i\hat{y}) \\ \mathbf{N}'^{(4)}_{lm} &= -\ (-1)^l\ l(l+1)\ \frac{1}{2}\ \frac{1}{kd}\ \partial_d [d\ h_l^{(2)}(kd)]\ (\hat{x} \pm i\hat{y}), \end{aligned}\right\} \tag{3.60}$$

which reduces to (3.1) and (3.2) with $z = 0$ if we retain only the first term in the finite series expansion of the spherical Hankel function (i.e. the zero order approximation). Using (3.49) and (3.60) in (3.51) we can show that

$$\mathbf{E}^{\text{inc}}_{B\to A}(r{=}0) = ip\ (\hat{x} \pm i\hat{y})\ W_1(kd)\ \left\{\chi_1(ka) - i\sum_{n=1}^{\infty} \frac{1}{n!\ (i2kd)^n}\left[\eta_n(ka) + \frac{1}{kd}\,\mathfrak{N}_n(ka)\right]\right\} \tag{3.61}$$

where

$$\left.\begin{aligned}\eta_n(\zeta) &= -\sum_{l=|n|}^{\infty}(-1)^l\ (2l+1)\ \frac{(l+|n|)!}{(l-|n|)!}\ \frac{1}{\zeta h_l^{(2)}(\zeta)\ \partial_\zeta[\zeta h_l^{(2)}(\zeta)]}\\ \mathfrak{N}_n(\zeta) &= |n|\sum_{l=|n|}^{\infty}(-1)^l\ (2l+1)\ \frac{(l+|n|)!}{(l-|n|)!}\ \frac{\partial_\zeta[\zeta j_l(\zeta)]}{\partial_\zeta[\zeta h_l^{(2)}(\zeta)]}.\end{aligned}\right\} \tag{3.62}$$

The reason for using $|n|$ instead of n will become apparent in chapter 4. Using asymptotic formulas like (3.26) we can show that for $l\to\infty$ (and $l\geq n$) the ratio of the $(l-n+2)^{\text{th}}$ term to the $(l-n+1)^{\text{th}}$ term for both series in (3.62) is $-\frac{(l+n+1)}{(l-n+1)}\left[\frac{\zeta}{2l}\right]^2 \to 0$. Thus the series in (3.62) are absolutely convergent for any finite ζ not at a pole of $\chi_1(\zeta)$. Furthermore, as $n\to\infty$ only the first term in either series contributes to that sum. Thus we have for $n\to\infty$

$$\frac{\eta_{n+1}}{\eta_n} \approx \frac{\mathfrak{N}_{n+1}}{\mathfrak{N}_n} \approx -\frac{\zeta^2}{2} = \text{const.} \tag{3.63}$$

Obviously, then, the sum over n in (3.61) is absolutely convergent. In particular, for $|kd| = \infty$ the sum vanishes and, using (3.48), $\mathbf{E}^{\text{inc}}_{B\to A}(r{=}0)$ reduces to what we had in (3.54) based on a zero order approximation.

For kd large but finite we retain the one dominant term in that sum and write

$$\mathbf{E}^{\text{inc}}_{B\to A}(r{=}0) \approx i\ p\ (\hat{x} \pm i\hat{y})\ W_1(kd)\left[\chi_1(ka) - \frac{\eta_1(ka)}{2kd}\right], \tag{3.64}$$

where $\eta_1(ka)$ is very similar in nature to $\chi_1(ka)$ [see (3.25)], but of course does not

have the same zeros. Let $k = k_0 + \Delta k$, where $\chi_1(k_0 a) = 0$ and $|\Delta k/k_0| \ll 1$, so that to first order in Δk $\quad \chi_1(ka) = \chi'_1(k_0 a)\, \Delta ka$, where the prime indicates differentiation. Comparing (3.64) with (3.54) we then write

$$\Delta ka \approx \frac{1}{\chi'_1(k_0 a)} \left[\frac{p}{W_1(k_0 d)} + \frac{\eta_1(k_0 a)}{2k_0 d} \right] \approx \frac{1}{2k_0 d} \frac{\eta_1(k_0 a)}{\chi'_1(k_0 a)} = O\left[\frac{1}{k_0 d} \right] \quad (3.65)$$

since the second term dominates as $|k_0 d| \to \infty$. This latter observation implies that the parity degeneracy of (3.31) is not lifted to first order in $1/kd$.

From (3.65) we see that any correction to our earlier results is of order $1/kd$ which vanishes in the limit $d \to \infty$. Thus we have shown that the natural frequencies and coefficients for the natural modes derived for the zero order approximation of the multipole fields also work for the exact multipole fields in the limit $d \to \infty$, at least at the point $r=0$. (The tedious generalization to include a neighborhood of sphere A should be straightforward, but we forsake it in place of a proper first order correction). This is simply a double-check on the validity of using asymptotic approximations from the beginning, instead of first solving the problem exactly and then taking the limiting form of the solution as $d \to \infty$. Within the limits of this derivation, both methods produce the same result.

Now let us begin a systematic first order correction. In order to determine the new translation coefficients we need asymptotic expansions for $\mathbf{M}'^{(4)}_{lm}$ and $\mathbf{N}'^{(4)}_{lm}$ in the neighborhood of sphere A, where

$$\left.\begin{aligned} r' &= d - z + \frac{\rho^2}{2d} + O(d^{-2}); \quad \rho^2 = x^2 + y^2 \\ \pi - \theta' &= \frac{\rho}{d}\left[1 + \frac{z}{d} + O(d^{-2})\right] \\ \phi' &= \phi. \end{aligned}\right\} \tag{3.66}$$

Using (3.66), (2.3) and the formulas in the Appendix we can show that, correct to first order in $1/kd$ $(m = \pm 1)$

$$\mathbf{M}'^{(4)}_{lm} = \pm\, i^{-l+1}\, l(l+1)\, W_1(kd)\left[e^{ikz}\,(\hat{x} \pm i\hat{y}) + \frac{1}{kd}\,\mathbf{S}_{lm}\right] \tag{3.67a}$$

$$\mathbf{N}'^{(4)}_{lm} = \pm\, \mathbf{M}'^{(4)}_{lm}, \quad \text{where} \tag{3.67b}$$

$$\mathbf{S}_{lm} = \left[(\hat{x} \pm i\hat{y})\left(\frac{l(l+1)}{i2} + kz + \frac{k^2\rho^2}{i2}\right) + \hat{z}\, k\rho e^{\pm i\phi}\right] e^{ikz}. \tag{3.67c}$$

Compare (3.67) with (3.1) and (3.2). In particular, notice that (3.67b) implies that (3.3) still holds so we see that the form, or structure of the matrix equations (3.12) is insensitive to first order corrections. This is a happy circumstance.

It is easy to verify that $\mathbf{M}'$ and $\mathbf{N}'$ in (3.67) are solenoidal [and satisfy (2.2)]. Thus we attempt an expansion in the form of (2.5), with due regard to (3.3). In (3.67a) we already know the expansion of the zero order term (3.1), so we consider the first order term

$$\begin{aligned} \mathbf{S}_{lm} = &\left[(\hat{r}\sin\theta + \hat{\theta}\cos\theta \pm i\hat{\phi})\left(\frac{l(l+1)}{i2} + kr\cos\theta + \frac{k^2r^2\sin^2\theta}{i2}\right)\right. \\ &\left. + (\hat{r}\cos\theta - \hat{\theta}\sin\theta)\, kr\, \sin\theta\right] e^{\pm i\phi}\, e^{ikr\cos\theta} \\ = &\sum_{\nu=1}^{\infty} C_\nu^{\pm}\left[\mathbf{M}^{(1)}_{\nu m} \pm \mathbf{N}^{(1)}_{\nu m}\right]. \end{aligned} \tag{3.68}$$

As in section 3.1, the radial component of this equation provides enough information

to solve for the $C_\nu^\pm$. Using (3.6), (2.3) and some recurrence relations for the Legendre and spherical Bessel functions we find

$$C_\nu^\pm = -+ \frac{1}{2}\, i^\nu\, \frac{(2\nu+1)}{\nu(\nu+1)}\, [(\nu-1)(\nu+2) + l(l+1)]. \tag{3.69}$$

Combining this intermediate result with (3.67a) and the first of (3.9) we can summarize the results for the first order translation coefficients as follow:

$$\left.\begin{aligned} \alpha_{lm}^{\nu m} &= i^{l-\nu} \frac{(2l+1)}{l(l+1)}\, \nu(\nu+1)\, W_1(kd) \left\{1 + \frac{[(l-1)(l+2) + \nu(\nu+1)]}{i\,2kd}\right\} \\ \beta_{lm}^{\nu m} &= \pm\alpha_{lm}^{\nu m} \\ \alpha'^{\nu m}_{lm} &= (-1)^{l-\nu}\alpha_{lm}^{\nu m} \\ \beta'^{\nu m}_{lm} &= -\,(-1)^{l-\nu}\beta_{lm}^{\nu m} \end{aligned}\right\} \tag{3.70}$$

Compare these equations with their zero order counterparts (3.9).

As mentioned already, the structure of the matrix equations (3.12) is unaltered. In fact, the entire discussion in section 3.2 is directly applicable to the first order case presently under consideration, except for an obvious modification of the matrix elements in (3.10), with a corresponding modification of (3.21), namely

$$\left.\begin{aligned} U_{l1} &= i^l\, \frac{(2l+1)}{l(l+1)} \left[1 + \frac{(l-1)(l+2)}{i\,2kd}\right] \\ V_{\nu 1} &= i^{-\nu}\, \nu(\nu+1) \left[1 + \frac{\nu(\nu+1)}{i\,2kd}\right]. \end{aligned}\right\} \tag{3.71}$$

These will generate the translation (matrix) operators correct to first order in $1/kd$.

The transcendental equation (3.24) has the same form, but now

$$\chi_1(\zeta) = i\sum_{l=1}^{\infty} (-1)^l\, (2l+1) \left\{1 - \frac{i}{kd}\, [l(l+1) - 1]\right\} \frac{1}{\zeta h_l^{(2)}(\zeta)\, \partial_\zeta[\zeta h_l^{(2)}(\zeta)]}, \tag{3.72}$$

which follows from using (3.71) above in (3.23). For $d \to \infty$ this χ_1 reduces to its zero

order counterpart (3.25), and the natural frequencies are as shown in Fig. 2 (for case $a = b$). With the first order correction we should be able to determine the paths that the natural frequencies follow in the complex plane as we reduce d from an infinite value to a large, but finite value. The question is: What is the domain of $|kd|$ within which (3.72) is considered valid? Recall that retaining only the first two terms in the expansion of $h_l^{(2)}(kd)$ is a good approximation only when $|kd| \gg l(l+1)/2$ (see the Appendix). The same is true of (3.72); the first order term in braces is in the spirit of a small correction, and so must be much smaller than the zero order term, unity. Here we take $l = l_0$, where l_0 is the highest order term that still contributes significantly to the sum (3.72). Numerically we find l_0 ranges approximately between 5 and 10, at least for the first few natural frequencies. This means, even in the best case, $|kd| \gg 15$, say $|kd| > 100$. Then the first order correction for the (dominant) $l = 1$ term in (3.72) is of order one percent, and the factor $W_1(kd)$ is practically zero. Thus we cannot, with any confidence, venture very far from the $d \to \infty$ limiting case.

Nevertheless, we can use the first order information to calculate exactly the "angle of departure", to borrow a term from control system theory. This is the angle that the tangent to the natural frequency path makes with the positive real axis in the $d \to \infty$ limit, i.e., the initial direction the path takes as d is made finite. Using (3.62) we can rewrite (3.72) as

$$\chi_1(\zeta) = \left[1 + \frac{i}{kd}\right] \chi_1^{(0)}(\zeta) - \frac{1}{kd}\,\eta_1(\zeta), \tag{3.73}$$

where $\chi_1^{(0)}$ is the zero order approximation (3.25). For d large let us set $k = k_0 + \Delta k$, where $|\Delta k/k_0| \ll 1$ and $\chi_1^{(0)}(k_0 a) = 0$, so that $\chi_1^{(0)}(ka) \approx \chi_1^{(0)\prime}(k_0 a)\,\Delta ka$, the prime indicating differentiation. In the case $a = b$ the transcendental equation tells us

$\chi_1(ka) = p/W_1(kd)$ [see (3.48)]. Using this information in (3.73) and taking the limiting form as $d \to \infty$ we find

$$\Delta ka = \frac{1}{k_0 d} \frac{\eta_1(k_0 a)}{\chi_1^{(0)\prime}(k_0 a)} = O\left[\frac{1}{k_0 d}\right]. \tag{3.74}$$

The angle of departure is the angle of the complex number Δk, plus 90 degrees, which is a function of the particular natural frequency $s_0 = ik_0 c$.

Notice that the angle of departure is independent of the parity p, as predicted in (3.65). This means the paths of the symmetric/antisymmetric pairs coalesce in the limit $d \to \infty$. (Both approach the limit point from the same angle). Notice also that (3.74) is single-valued, which implies that the number of natural oscillations is a conserved quantity, i.e., invariant to changes in d, at least to the order of these approximations. Using (3.28) it is easy to verify that if k_0 is replaced with $-k_0^*$, then Δk is replaced with $-\Delta k^*$, indicating that each path in the complex frequency plane has a complex conjugate dual, as expected. Furthermore, the magnitude of Δkd is a measure of how rapidly the natural frequencies depart from their $d \to \infty$ limiting values as d is made finite. In this sense Δkd in (3.74) can be thought of as a "departure vector" (angle and magnitude). Finally, compare (3.74) with our earlier estimate (3.65); the extra 1/2 in (3.65) is rooted in the fact that we allowed only k to have a first order correction - actually both k and the natural mode coefficients undergo a first order perturbation.

Fig. 3 is similar to Fig. 2, augmented with the first order information. The short line segment emanating from a zero order natural frequency is at the departure angle, and has magnitude proportional to the departure vector.

Some general observations: The departure angle lies between about -90 and -180 degrees. Thus the initial perturbation of the natural frequencies as the spheres are

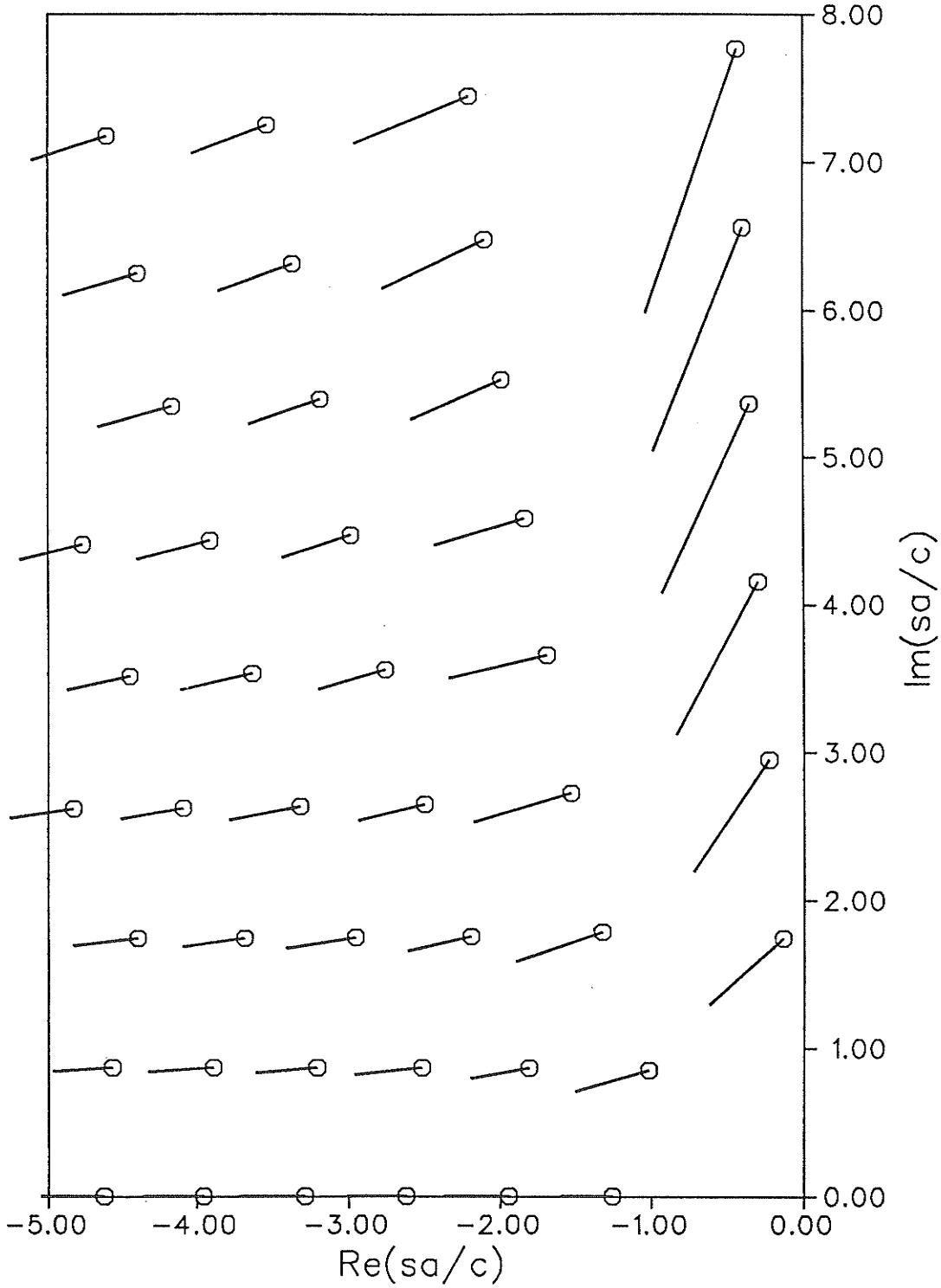

Fig 3: Natural frequencies and departure vectors for $d \to \infty$, $a=b$, $m=\pm 1$.

brought closer together results in decrease frequency ω and increased damping rate $|\Omega|$. The relative importance of these two changes depends on the departure angle. For example, for rapid (large ω) high Q (small $|\Omega|$) free oscillations the departure angle is closest to -90 degrees; the initial perturbation is dominated by a change in frequency ω over change in damping rate. Furthermore, the overall magnitude of the departure vector tends to be largest in this case. On the other hand, the natural frequencies on the real axis can only change in damping coefficient Ω, and so have a departure angle equal to -180 degrees. (Of course zero degrees is also conceivable, but does not seem to occur in reality). A change in frequency ω is not possible because of conservation of number of free oscillations, and the fact that $|\chi_1|$ is symmetric with respect to the real s-axis.

The natural mode coefficients are still given by (3.45), where the U_{l1} are now given by (3.71) instead of (3.21). Recall the extra 1/2 in (3.65). We derived this result under the simple-minded assumption that B^E and B^H in (3.49) were the same as in the zero order case; then (3.65) was the first order correction to k necessary to produce the desired result (3.54) (with $z = 0$). It can be shown that if we were to repeat the derivation, but this time using the first order correct B^E and B^H we would find the correction to k given by (3.74) instead of (3.65).

Recall that in our discussion of the natural modes in section 3.4 we described the behavior of the fields on the axis connecting the two spheres. In particular, $\mathbf{E}^{\text{inc}}_{B\to A}$ given in (3.54) is correct in the neighborhood of sphere A in the limit $d\to\infty$. What can our first order corrections tell us about the interaction fields for d large but finite, especially the paraxial behavior? In general

$$\mathbf{E}^{\text{inc}}_{B\to A} = \sum_{l=1}^{\infty} \left[B^E_{lm}\mathbf{N}'^{(4)}_{lm} + B^H_{lm}\mathbf{M}'^{(4)}_{lm} \right]. \tag{3.75}$$

Using the multipole fields in (3.67) and the B coefficients in (3.49) for the case $a = b$ this becomes

$$\mathbf{E}^{\text{inc}}_{B\to A} = i\ e^{ikz}\left\{(\hat{x} \pm i\hat{y})\left[1 + \frac{1}{d}\left[z - ik\frac{\rho^2}{2}\right]\right] + \hat{z}\ \frac{1}{d}\ (x \pm iy)\right\}, \qquad (3.76)$$

which is valid in the neighborhood of sphere A and up to first order in $1/kd$. Note that $(x \pm iy) = \rho e^{\pm i\phi}$ and $(\hat{x} \pm i\hat{y}) = (\hat{\rho} \pm i\hat{\phi})\ e^{\pm i\phi}$, showing explicitly the $e^{im\phi}$ azimuthal dependence. Compare (3.76) with its zero order counterpart (3.54) obtained by letting $d \to \infty$.

On the $\rho = 0$ axis (3.76) reduces to the usual (3.54) times the first order correction factor

$$\frac{d}{r'} = 1 + \frac{z}{d} + O\,(d^{-2}), \qquad (3.77)$$

where r' is the distance from the center of sphere B to the observation point. This correction comes from the inverse distance factor common to all spherical waves. If $z = 0$ also, then $r = 0$ and $\mathbf{E}^{\text{inc}}_{B\to A}$ of course reduces to $i\ (\hat{x} \pm i\hat{y})$.

For the paraxial case let us first rewrite $\mathbf{E}^{\text{inc}}_{B\to A}$ in the more revealing form

$$\mathbf{E}^{\text{inc}}_{B\to A} = \frac{1}{2W_1(kd)}\ (\hat{\theta}' \mp i\hat{\phi}')\ e^{\pm i\phi'}\ \frac{e^{-ikr'}}{kr'}, \qquad (3.78)$$

which, when expanded in powers of $1/d$ reduces to (3.76), correct up to first order terms. Recall that the primes here refer to the O' coordinate system centered on sphere B. The origins of the various factors in (3.78) are suggested by inspection of the multipole fields (2.3) and the limiting forms for the Legendre functions as $\theta' \to \pi$, particularly the transverse (to $\hat{r}'$) polarization term $(\hat{\theta}' \mp i\hat{\phi}')\ e^{im\phi'}$. The radial dependence is clearly a spherical wave, whose exponentially large magnitude in the region of sphere A is tamed by the factor $[W_1(kd)]^{-1}$ - a direct manifestation of the

destructive interference process.

Unfortunately $| \mathbf{E}^{\text{inc}}_{B\to A} |$ in (3.78) does not exhibit any dependence on θ'; to this order of approximation $| \mathbf{E}^{\text{inc}}_{B\to A} |$ is spherically symmetrical about O', at least in its intended domain, and so does not reveal any interesting paraxial behavior. As expected, in this $| m | = 1$ case θ' dependence is a second order effect [see (A.3) and (A.4) of the Appendix]. Nevertheless, we can speculate with great confidence that for $r' \approx d$ ($r \approx d$) the magnitude of the field radiated by sphere B (A) has a sharp global minimum at $\theta' = \pi$ ($\theta = 0$); the conditions for appreciable destructive interference are not satisfied elsewhere. Together with our previous discussion about the behavior of the fields on the axis connecting the two spheres (section 3.4), we can now envision the energy density being at a minimum in the vicinity of the spheres, and (more or less) increasing with radial distance from either sphere. This is consistent with energy being radiated out to infinity with the passage of time.

The calculation of second and higher order correction terms quickly becomes unwieldy. Most importantly, correction terms beyond first order destroy condition (3.3) and thus the simple coupling structure of (3.12) no longer obtains. Although these changes in coupling structure may provide useful physical insight, we have instead committed our time to the solution for cases $| m | \neq 1$.

CHAPTER 4: CASE $|\mathbf{m}| \geq 1$

In chapter 3 we discussed the case $|m| = 1$ in great detail. We now have a good understanding of the physical principles behind the free oscillations of the electromagnetic fields in the presense of two conducting spheres, at least for unity azimuthal number and large sphere separation. The case $|m| > 1$ is qualitatively the same in many ways, but there are some important differences. This brief chapter is a formal collection of the results for all cases $|m| \geq 1$, with an emphasis on these differences. The overlap with the $|m| = 1$ case provides a double-check of the results in chapter 3, since the two sets of results were actually derived independently of each other.

From the outset, all derivations and results in this chapter are correct to first order in $1/kd$. Notation: Because of cylindrical symmetry most quantities depend on $|m|$ rather than m, so we shall write ± 1 in place of $m/|m|$ to emphasize the dependence of this quantity on the sign of m. In other words, we have set $m \equiv \pm |m|$, which is consistent with the usage of the double sign in chapter 3.

4.1 Translation Coefficients

As in section 3.5 we can show that in the vicinity of sphere A [as defined in (3.66)]

$$\mathbf{M}'^{(4)}_{lm} = \pm\, i^{-l+|m|}\, \frac{(l+|m|)!}{(l-|m|)!}\, W_m(kd) \cdot \left\{ (k\rho e^{\pm i\phi})^{|m|-1}\, e^{ikz}\, (\hat{x} \pm i\hat{y}) + \frac{1}{kd}\, \mathbf{S}_{lm} \right\} \tag{4.1a}$$

$$\mathbf{N}'^{(4)}_{lm} = \pm\, \mathbf{M}'^{(4)}_{lm}, \quad \text{where} \tag{4.1b}$$

$$S_{lm} = \left[(\hat{x} \pm i\hat{y}) \left[\frac{l(l+1)}{i2} + |m|\, kz + \frac{k^2\rho^2}{i2} \right] + \hat{z}\, k\rho e^{\pm i\phi} \right] \cdot (k\rho e^{\pm i\phi})^{|m|-1} e^{ikz} \tag{4.1c}$$

$$W_m(kd) = \frac{i^{|m|}}{2^{|m|}\,(|m|-1)!} \frac{e^{-ikd}}{(kd)^{|m|}}, \tag{4.1d}$$

all correct to first order in $1/kd$. Compare (4.1) with (3.67), to which it reduces in the case $m = \pm 1$. The most important difference is the $(k\rho e^{\pm i\phi})^{|m|-1} = [k\ (x \pm iy)]^{|m|-1}$ factor, which makes even the zero order multipole fields in this region nonuniform helical waves for $|m| > 1$, as opposed to uniform plane waves for $|m| = 1$. This will of course directly affect the form of the interaction fields $\mathbf{E}^{\text{inc}}_{B\to A}$ and $\mathbf{E}^{\text{inc}}_{A\to B}$ (discussed in section 4.3). For $|m| > 1$ $\mathbf{M}'$ and $\mathbf{N}'$ vanish on the axis connecting the two spheres, which we originally suspected may make the coupling weak or even negligible. Furthermore, notice the extra inverse $(kd)^{|m|-1}$ factor in W_m over the W_1 case. However, we now know that the strength of coupling is dominated by the exponential growth factor in $W_m(kd)$, so that the individual partial waves striking the spheres still have enormous amplitudes, except in an "epsilon neighborhood" of the axis.

As a double-check we can verify that the $\mathbf{M}'$ and $\mathbf{N}'$ in (4.1) are solenoidal and satisfy (2.2). (4.1b) implies, as might have been expected, that (3.3) holds for all $|m| \geq 1$, namely

$$\beta^{lm}_{\nu m} = \pm\, \alpha^{lm}_{\nu m}. \tag{4.2}$$

As usual, this allows us to write

$$\hat{r} \cdot \mathbf{M}'^{(4)}_{lm} = \pm \sum_{\nu=|m|}^{\infty} \alpha^{lm}_{\nu m}\, \hat{r} \cdot \mathbf{N}'^{(1)}_{\nu m}. \tag{4.3}$$

Setting

$$\alpha^{lm}_{\nu m} \equiv i^{-l+|m|}\, \frac{(l+|m|)!}{(l-|m|)!}\, \frac{1}{\nu(\nu+1)}\, W_m(kd)\, \left[C^{(0)}_\nu + C^{(1)}_\nu\right], \tag{4.4}$$

in (4.3) and rearranging yields

$$\begin{aligned} &\left\{(kr\sin\theta)^{|m|}\, e^{ikr\cos\theta} + \frac{1}{kd}\, \left[(kre^{-im\phi})\, \hat{r} \cdot \mathbf{S}_{lm}\right]\right\} \\ &\qquad = \sum_{\nu=|m|}^{\infty} \left[C^{(0)}_\nu + \frac{1}{kd}\, C^{(1)}_\nu\right] j_\nu(kr)\, P^m_\nu(\cos\theta), \end{aligned} \tag{4.5}$$

where $C^{(0)}_\nu$ and $C^{(1)}_\nu$ are unknown coefficients to be determined.

. For the zero order part of (4.5) we write

$$\begin{aligned} L.H.S. &= i^{-|m|}\, (\sin\theta)^{|m|}\, \frac{d^{|m|}}{d(\cos\theta)^{|m|}}\, e^{ikr\cos\theta} \\ &= i^{-|m|} \sum_{\nu=|m|}^{\infty} i^\nu\, (2\nu+1)\, j_\nu(kr)\, P^m_\nu(\cos\theta), \end{aligned}$$

where we made use of (3.6). Thus

$$C^{(0)}_\nu = i^{\nu-|m|}\, (2\nu+1). \tag{4.6}$$

For the first order part of (4.5) we write [see (4.1c)]

$$L.H.S. = \frac{1}{kd}\, \left[\frac{l(l+1)}{i2} + (|m|+1)\, kr\cos\theta + \frac{(kr\sin\theta)^2}{i2}\right] (kr\sin\theta)^{|m|}\, e^{ikr\cos\theta}$$

where the factor $(kr\sin\theta)^{|m|}\, e^{ikr\cos\theta}$ is the same as the zero order part. After a couple of pages of tedious algebra and recurrence relations we find

$$C^{(1)}_\nu = C^{(0)}_\nu\, \frac{[l(l+1) + (\nu-|m|)(\nu+|m|+1)]}{i2} \tag{4.7}$$

Using (4.6) and (4.7) in (4.4) finally yields $\alpha^{lm}_{\nu m}$.

The translation coefficients are summarized below:

$$\left.\begin{aligned}
\alpha_{lm}^{\nu m} &= i^{l-\nu}\,\frac{(2l+1)}{l(l+1)}\,\frac{(\nu+|m|)!}{(\nu-|m|)!}\,W_m(kd)\left\{1+\frac{[(l-|m|)(l+|m|+1)+\nu(\nu+1)]}{i2kd}\right\}\\
\beta_{lm}^{\nu m} &= \pm\,\alpha_{lm}^{\nu m}\\
\alpha'^{\nu m}_{lm} &= (-1)^{l-\nu}\,\alpha_{lm}^{\nu m}\\
\beta'^{\nu m}_{lm} &= -(-1)^{l-\nu}\,\beta_{lm}^{\nu m}
\end{aligned}\right\} \tag{4.8}$$

Compare these equations with (3.70) for $|m| = 1$. As mentioned already, the extra inverse $(kd)^{|m|-1}$ in W_m over W_1 makes the coupling slightly weaker, but by no means negligible!

Again the entire discussion of the solution in section 3.2 applies, in spirit, to the present case, with obvious modifications in notation to accommodate the increased generality $|m| \geq 1$. For example, W_1 becomes W_m, et cetera. Further, (3.21) becomes

$$\left.\begin{aligned}
U_{lm} &= i^{l}\,\frac{(2l+1)}{l(l+1)}\left[1+\frac{(l-|m|)(l+|m|+1)}{i2kd}\right]\\
V_{lm} &= i^{-\nu}\,\frac{(\nu+|m|)!}{(\nu-|m|)!}\left[1+\frac{\nu(\nu+1)}{i2kd}\right].
\end{aligned}\right\} \tag{4.9}$$

Compare these with (3.71) for $|m| = 1$. By (4.9) and (3.17) we have

$$\chi_m(\zeta) = V_m^T\,\Gamma(\zeta)\,U_m = \sum_{l=|m|}^{\infty} U_{lm}\,V_{lm}\,\Gamma_l(\zeta) \tag{4.10}$$

$$= i\sum_{l=|m|}^{\infty}(-1)^{l+m-1}\,\frac{(2l+1)}{l(l+1)}\,\frac{(l+|m|)!}{(l-|m|)!}$$

$$\cdot\left[1+\frac{2l(l+1)-|m|(|m|+1)}{i2kd}\right]\frac{1}{\zeta h_l^{(2)}(\zeta)\,\partial_\zeta[\zeta h_l^{(2)}(\zeta)]},$$

which is to be compared with (3.72). The transcendental equation for the natural

frequencies is

$$[W_m(kd)]^2\, \chi_m(ka)\, \chi_m(kb) = 1, \tag{4.11}$$

an obvious generalization of (3.24).

4.2 Natural Frequencies

In the limit $d \to \infty$ we write, in the usual notation,

$$\chi_m(\zeta) \to \chi_m^{(0)}(\zeta) = i \sum_{l=|m|}^{\infty} (-1)^{l+m-1} \frac{(2l+1)}{l(l+1)} \frac{(l+|m|)!}{(l-|m|)!} \cdot \frac{1}{\zeta h_l^{(2)}(\zeta)\, \partial_\zeta [\zeta h_l^{(2)}(\zeta)]}. \tag{4.12}$$

$\chi_m^{(0)}$ is qualitatively very similar to $\chi_1^{(0)}$, the most important difference being the locations of the zeros (all of which are first order, as in the $|m| = 1$ case). We know that in the limit $d \to \infty$, k in the lower half complex plane means $W_m(kd) \to 0$ so, by (4.11), $\chi_m^{(0)}(kr) \to \infty$, where $r = a$ or b. But $\chi_m^{(0)}(\zeta)$ has the same poles as $\chi_1^{(0)}(\zeta)$ - only in the upper half ζ-plane, and at all other points in the finite ζ-plane the series in (4.12) is absolutely convergent (easily proven as in section 3.3). Thus there are no solutions to (4.11) for k in the lower half plane (s in the right half plane). The reason we emphasize this fact is that, unlike χ_1, χ_m ($|m| > 1$) apparently has some of its zeros in the *lower* half ζ-plane. Usually, singular points in the mathematics (like zeros) indicate important physical phenomena; in this case, however, these lower half plane zeros appear to have no physical meaning. (Indeed, if they *were* solutions they would imply free oscillations which grow exponentially with time).

Of course the zeros of $\chi_m^{(0)}(\zeta)$ in the *upper* half ζ-plane still furnish the natural frequencies through (3.32) (for case $a = b$ and $d \to \infty$). For brevity, in this chapter we consider only the case $a = b$; the case $a \neq b$ is a straightforward extension of these results [see chapter 3, in particular (3.43)].

As in the case $|m| = 1$, the usefulness of the first order correction term in (4.10) is practically limited to determination of the departure vector. Inspection of (3.62) reveals that we can rewrite (4.10) as

$$\chi_m(\zeta) = \left[1 - \frac{|m|(|m|+1)}{i2kd}\right] \chi_m^{(0)}(\zeta) - \frac{(-1)^{|m|-1}}{kd} \eta_m(\zeta). \tag{4.13}$$

In analogy with the $|m| = 1$ case, we set $k = k_0 + \Delta k$, where k_0 is a solution when $d \to \infty$, and find that in the limit of large d

$$\Delta ka = \frac{(-1)^{|m|-1}}{k_0 d} \frac{\eta_m(k_0 a)}{\chi_m^{(0)\prime}(k_0 a)} = O\left[\frac{1}{k_0 d}\right]. \tag{4.14}$$

Compare this with (3.74). Notice that the departure vector Δkd does not depend on the sign of m, in accordance with the basic degeneracy over sign of m; nor does it depend on the parity p. Incidentally, for the purpose of calculating (4.14) we find for the derivative of $\chi_m^{(0)}(\zeta)$:

$$\chi_m^{(0)\prime}(\zeta) = -i \sum_{l=|m|}^{\infty} (-1)^{l+m-1} \frac{(2l+1)}{l(l+1)} \frac{(l+|m|)!}{(l-|m|)!} \tag{4.15}$$

$$\cdot \left\{ \frac{[l(l+1)\zeta^{-2} - 1]}{[\partial_\zeta[\zeta h_l^{(2)}(\zeta)]]^2} + \frac{1}{[\zeta h_l^{(2)}(\zeta)]^2} \right\}.$$

Figs. 4, 5 and 6 are the same as Fig. 3, except they show the natural frequencies and departure vectors for $|m| = 2$, 3, and 4, respectively. We must stress that in these figures we are actually showing the zeros of $\chi_m^{(0)}$; as discussed already, only the zeros in the left half s-plane can be considered natural frequencies, the others are

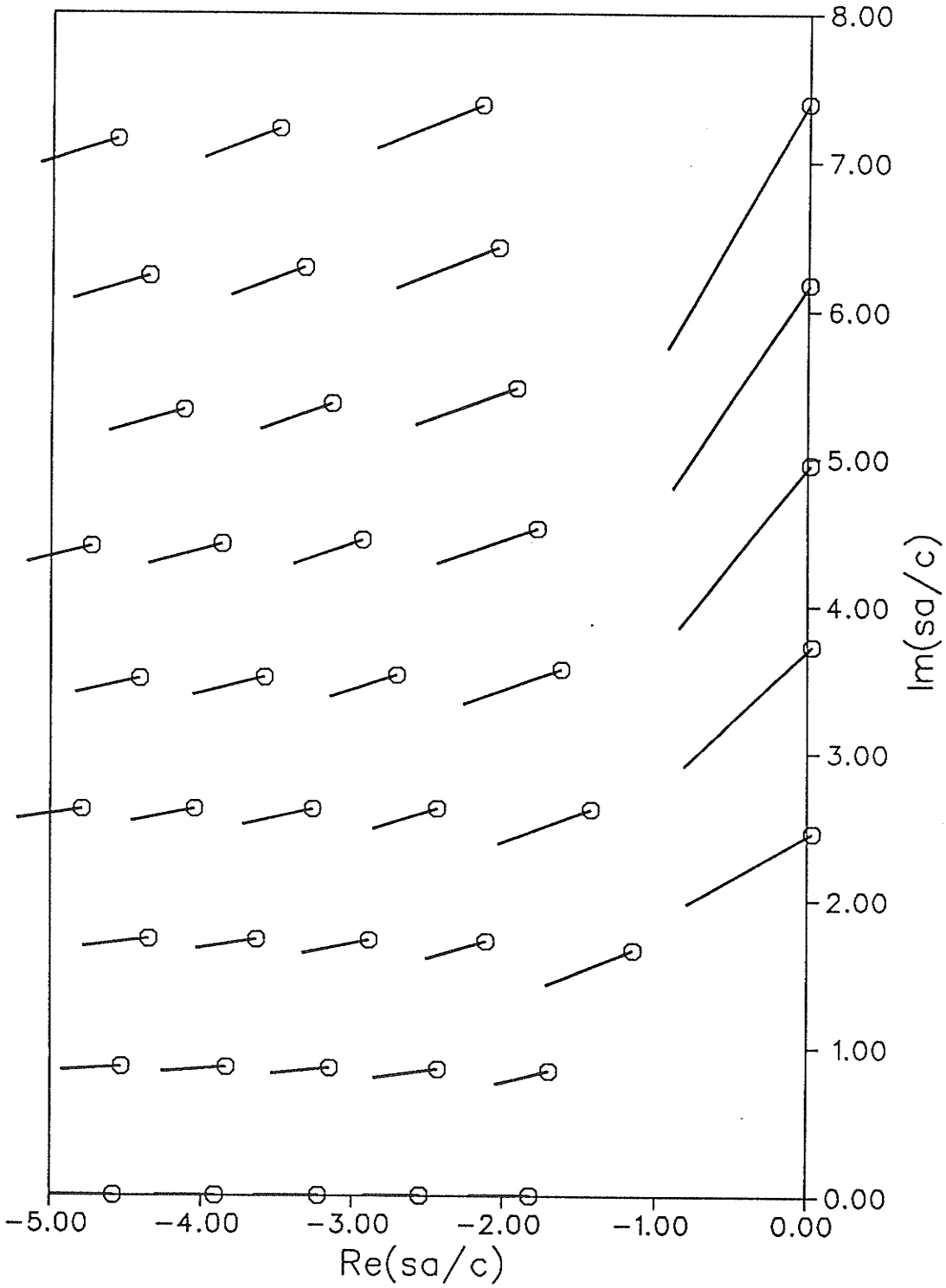

Fig 4: Natural frequencies and departure vectors for $d \to \infty$, $a=b$, $m=\pm 2$.

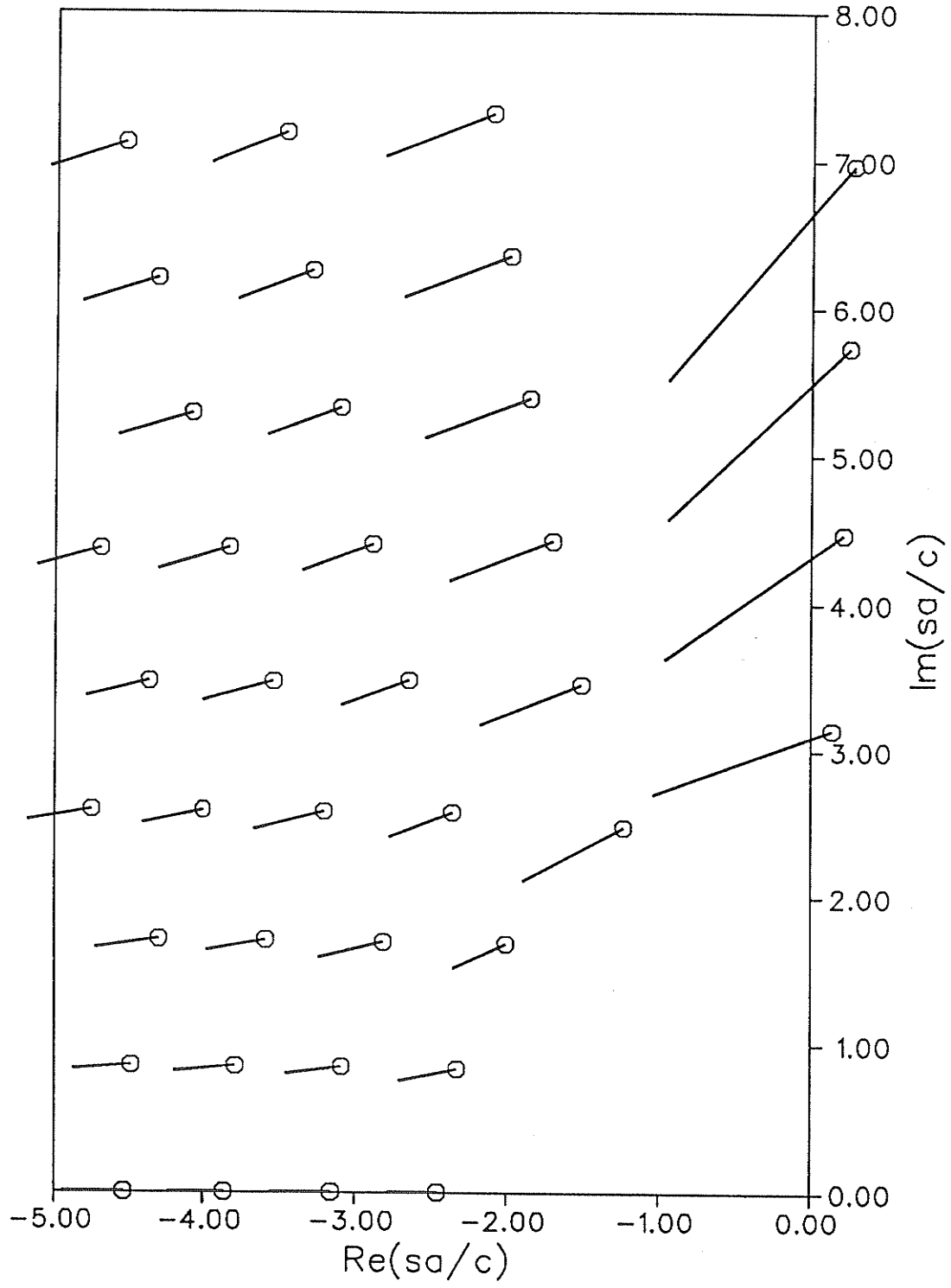

Fig 5: Natural frequencies and departure vectors for $d \to \infty$, $a=b$, $m=\pm 3$.

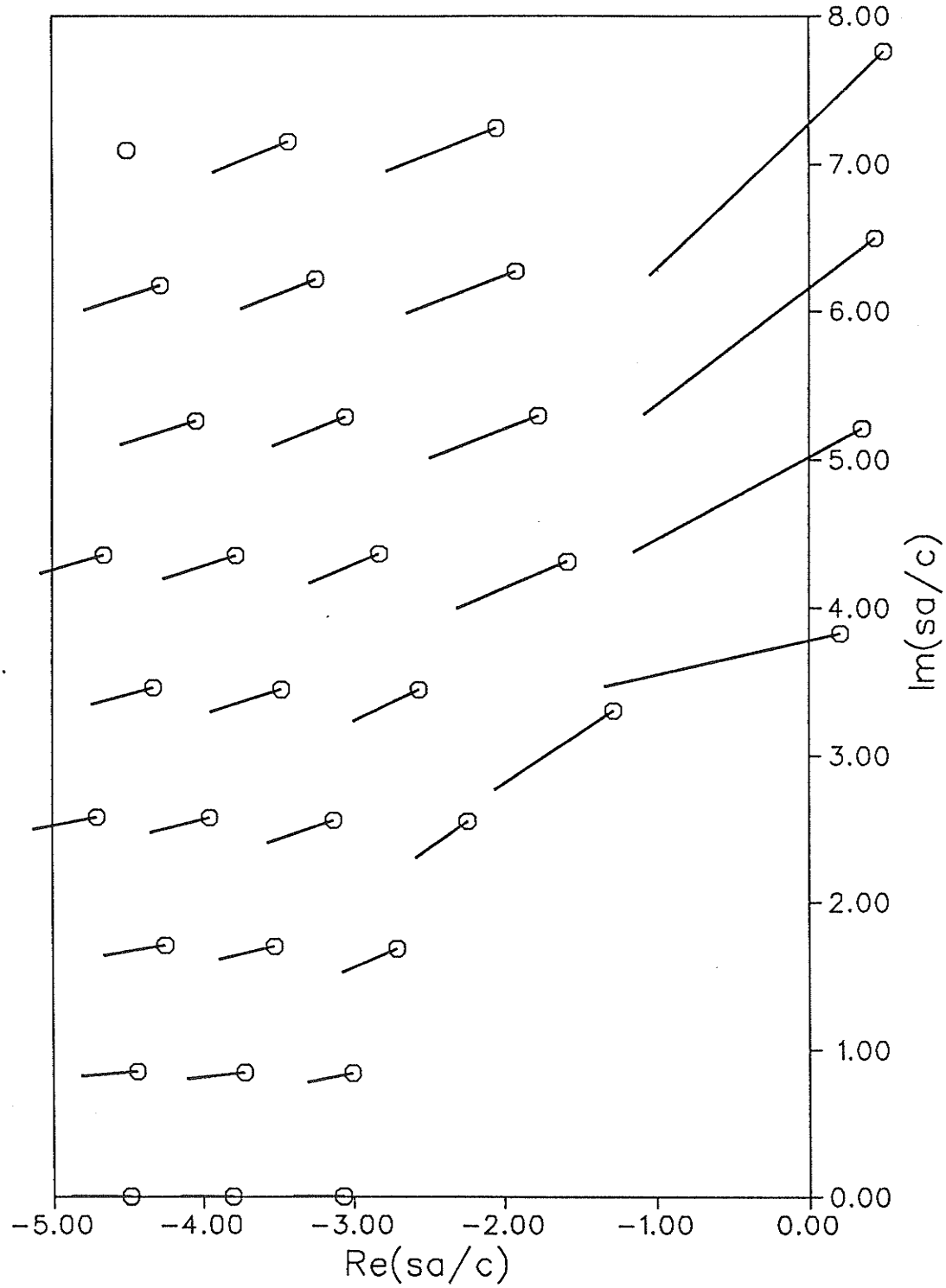

Fig 6: Natural frequencies and departure vectors for $d \to \infty$, $a=b$, $m=\pm 4$.

apparently meaningless. The reason for their inclusion will become clear in chapter 6 where we compare all m cases in detail.

Figs. 3 to 6 are qualitatively similar except for two general differences. The first is the migration of the first layer zeros towards and into the right half s-plane with increasing $|m|$. For $|m| = 1$ all of the first layer zeros of $\chi_1^{(0)}$ are in the left half plane and hence constitute natural frequencies. For $|m| = 2$ the first four zeros of $\chi_2^{(0)}$ are in the right half plane, but the fifth (and the sixth, and probably all higher ones not shown) lie in the left half plane. The numerical evaluation of $\chi_2^{(0)}$ (and all other $\chi_m^{(0)}$) was done very carefully to virtually rule out possibility of numerical error of any description. This "partially in the right and partially in the left half plane" behavior of the $|m| = 2$ first layer zeros is very curious indeed. For $|m| > 2$ all the first layer zeros appear to be in the right half plane; it is not known whether zeros higher in the layer eventually make their way back to the left half plane.

Inspection of Figs. 3 to 6 reveals an alternative way of classifying, or grouping the natural frequencies. Instead of layers, we notice approximate quarter-circle arcs centered about $s = 0$. In Fig. 3 the first arc has three natural frequencies, one being on the real axis. The second has four natural frequencies, and so on. Thus the second general difference between Figs. 3 to 6 is that the first arc starts further from the origin for increasing $|m|$. This behavior can be linked with the fact that the sum in (4.12) begins at $l = |m|$. The l^{th} term in this sum has poles that occur approximately in an arc (the electric and magnetic natural frequencies of a single sphere, see ahead to Fig. 10). The $l = 1$ arc is closest to the origin, and for $l = 2, 3, \cdots$ the arc radius is an increasing function of l. Thus the sum in (4.12) is missing the $l < |m|$ arcs of poles closest to the origin. The observed fact that the zeros of $\chi_m^{(0)}$ prefer to be interspersed amongst the poles then explains the aforementioned behavior.

We have discussed Figs. 3 to 6 in a rather descriptive way, preferring to leave the more meaningful speculation and physical insight to chapter 6, where we compare natural frequencies for all m cases.

4.3 Natural Modes

The natural mode coefficients are still given by (3.45), with U_1 replaced by U_m. Notice that the U_{lm} in (4.9) depends on $|m|$ only to first order, so in the limit $d \to \infty$ the form of the coefficients is independent of $|m|$ (but of course the values ultimately depend on the particular natural frequency and sign of m).

For the interaction fields we find

$$\mathbf{E}^{\text{inc}}_{B\to A} = i^{|m|}\,(k\rho e^{\pm i\phi})^{|m|-1}\,e^{ikz} \cdot \left\{(\hat{x} \pm i\hat{y})\left[1 + \frac{1}{d}\left[|m|\,z - ik\frac{\rho^2}{2}\right]\right] + \hat{z}\,\frac{1}{d}\,(x \pm iy)\right\}. \tag{4.16}$$

Compare this with (3.76). The most important difference is the factor $(k\rho e^{\pm i\phi})^{|m|-1}$ which, of course, makes even the zero order interaction fields nonuniform helical waves, just like the partial waves in (4.1). It is these differences in interaction fields for different $|m|$ which are responsible for the different sets of natural frequencies.

(4.16) can be written as

$$\mathbf{E}^{\text{inc}}_{B\to A} = \frac{(-1)^{|m|-1}}{2^{|m|}(|m|-1)!}\,\frac{1}{W_m(kd)}\,(\hat{\theta}' - i\hat{\phi}')\,e^{im\phi'}\,\frac{e^{-ikr'}}{kr'}\,(\sin\theta')^{|m|-1} \tag{4.17}$$

Compare this with (3.78). Recall that $\theta' \to \pi$ as in (3.66); the factor $(\sin\theta')^{|m|-1}$ dominates the paraxial behavior, and indicates the null that the natural modes have on the

axis connecting the two spheres when $|m| > 1$.

CHAPTER 5: CASE m = 0

Chapters 3 and 4 dealt in detail with the solution to the coupled equations (2.8) for the cases $|m| \geq 1$ and large sphere separation. Here we discuss the only remaining case, namely $m = 0$, wherein the fields have no azimuthal dependence. We shall see that the structure of the coupled equations (2.8) is markedly different from what we have seen before. In particular, the electric and magnetic multipole fields do not couple and so the natural modes are no longer hybrid. Some features of the solution will be familiar, but there are many interesting differences. As with chapter 4, this brief chapter is a formal collection of the results for the case $m = 0$, with an emphasis on its unique features; we shall try not to belabor the discussions of concepts already introduced. As usual, all calculations are carried out to first order in $1/kd$.

5.1 Translation Coefficients

For $m = 0$ the multipole fields in (2.3) reduce to

$$\left.\begin{aligned} \mathbf{M}_{l0}^{(j)} &= -\hat{\boldsymbol{\phi}}\, z_l^{(j)}(kr)\, \partial_\theta P_l(\cos\theta) \\ \mathbf{N}_{l0}^{(j)} &= \hat{\mathbf{r}}\, \frac{1}{kr}\, z_l^{(j)}(kr)\, l(l+1)\, P_l(\cos\theta) + \hat{\boldsymbol{\theta}}\, \frac{1}{kr}\, \partial_r [r z_l^{(j)}(kr)]\, \partial_\theta P_l(\cos\theta), \end{aligned}\right\} \quad (5.1)$$

where $l = 1, 2, \cdots$ As usual, we begin by finding expressions for the fields $\mathbf{M}'^{(4)}_{l0}$ and $\mathbf{N}'^{(4)}_{l0}$ emanating from origin O' (sphere B) in the vicinity of sphere A:

$$\mathbf{M}'^{(4)}_{l0} = \hat{\phi}\, i^{-l+1}\, l(l+1)\, W_0(kd)\, e^{ikz}\, k\rho \cdot \left[1 + \frac{1}{kd}\left[\frac{l(l+1)}{i2} + 2kz + \frac{k^2\rho^2}{i2}\right]\right] \tag{5.2a}$$

$$\mathbf{N}'^{(4)}_{l0} = (2\hat{z} - ik\rho\hat{\rho})\, i^{-l+1}\, l(l+1)\, W_0(kd)\, e^{ikz} \cdot \left[1 + \frac{1}{kd}\left[\frac{l(l+1)}{i2} + 2kz + \frac{k^2\rho^2}{i2} + \times\hat{\phi}k\rho\right]\right] \tag{5.2b}$$

where $\times\hat{\phi}$ means "cross-product with $\hat{\phi}$", and

$$W_0(kd) = -\frac{1}{2}\,\frac{e^{-ikd}}{(kd)^2}. \tag{5.2c}$$

Comparing (5.2) with (4.1) we see several similarities with cases $|m| = 1$ and 2, e.g., the $l(l+1)$ factor, the $k\rho$ factor in (5.2a), the $2kz$ term in the parentheses on the far right of (5.2a,b), and the inverse $(kd)^2$ factor in (5.2c). It must be stressed that these similarities are purely coincidental. The fact that the nature of the $m = 0$ case is fundamentally different from that of the $|m| \geq 1$ cases is based on the following observations: (i) all $m = 0$ fields have cylindrical symmetry about the axis joining the two sphere centers, (ii) $\mathbf{M}'$ and $\mathbf{N}'$ in (5.2) are linearly independent vector fields, as opposed to the simple relationship in (4.1b) (to this order of approximation), and (iii) W_m in (4.1d) does not extend naturally to the case $m = 0$; in fact $(-1)! = \Gamma(0)$ is not defined which, together with (ii), leads us to suspect (correctly) that the basic structure of the coupled equations (2.8) is not of the same form as (3.12). W_0 as defined in (5.2c) is completely independent of W_m defined in (4.1d).

In the vicinity of sphere A, and to zero order in $1/kd$, the magnetic multipole $\mathbf{M}'^{(4)}_{l0}$ is a transverse ($\hat{\phi}$ polarized) nonuniform plane wave which vanishes on the z-axis, whereas the electric multipole $\mathbf{N}'^{(4)}_{l0}$ is approximately a longitudinal (radially polarized) wave which does not vanish on the z-axis. It is easy to double-check that

both fields are solenoidal and satisfy (2.2). Thus we attempt the usual expansion

$$\mathbf{M}'^{(4)}_{l0} = \sum_{\nu=1}^{\infty} \left[\alpha^{l0}_{\nu 0} \mathbf{M}^{(1)}_{\nu 0} + \beta^{l0}_{\nu 0} \mathbf{N}^{(1)}_{\nu 0} \right]. \tag{5.3}$$

Examining the radial component of both sides of this equation reveals $\beta^{l0}_{\nu 0} = 0$ for all ν, l. Only a $\hat{\phi}$ component remains and we find, after some manipulations,

$$\left[1 + \frac{1}{kd} \left[\frac{l(l+1)}{i2} + 2kr\cos\theta + \frac{k^2 r^2 \sin^2\theta}{i2} \right] \right] \sum_{\nu=1}^{\infty} i^{\nu} (2\nu + 1)\, j_{\nu}(kr)\, P^{1}_{\nu}(\cos\theta)$$
$$= \sum_{\nu=1}^{\infty} \left[C_{\nu}(0) + \frac{1}{kd} C^{(1)}_{\nu} \right] j_{\nu}(kr)\, P^{1}_{\nu}(\cos\theta), \tag{5.4}$$

where we have set

$$\alpha^{l0}_{\nu 0} \equiv i^{-l}\, l(l+1)\, W_0(kd) \left[C^{(0)}_{\nu} + \frac{1}{kd} C^{(1)}_{\nu} \right] \tag{5.5}$$

and made use of (3.6) and the fact that $\partial_{\theta} P_{\nu}(\cos\theta) = - P^{1}_{\nu}(\cos\theta)$.

For the zero order part we obviously have

$$C^{(0)}_{\nu} = i^{\nu} (2\nu + 1). \tag{5.6}$$

For the first order part we can save ourselves some effort by recognizing the similarity with the case $| m | = 1$ [see the discussion following (4.6)]. Thus we have

$$C^{(1)}_{\nu} = C^{(0)}_{\nu} \frac{[l(l+1) + (\nu - 1)(\nu + 2)]}{i2} \tag{5.7}$$

the same as (4.7) (coincidentally).

The translation coefficients for $m = 0$ are summarized below:

$$\left.\begin{aligned}
&\alpha_{l0}^{\nu 0} = i^{l-\nu}\,(2l+1)\,\nu(\nu+1)\,W_0(kd)\left\{1+\frac{[(l-1)(l+2)+\nu(\nu+1)]}{i2kd}\right\}\\
&\alpha'^{\nu 0}_{l0} = (-1)^{l-\nu}\,\alpha_{l0}^{\nu 0}\\
&\beta_{l0}^{\nu 0} = 0 = \beta'^{\nu 0}_{l0}.
\end{aligned}\right\} \tag{5.8}$$

5.2 Solution of the Coupled Equations

As usual we define the matrix elements

$$\left.\begin{aligned}
F_{l0}^{\nu 0} &\equiv \frac{\alpha_{l0}^{\nu 0}}{W_0(kd)} = U_{l0}V_{\nu 0}\\
F'^{\nu 0}_{l0} &\equiv \frac{\alpha'^{\nu 0}_{l0}}{W_0(kd)} = (-1)^{l-\nu}\,F_{l0}^{\nu 0}
\end{aligned}\right\} \tag{5.9}$$

so that in matrix notation

$$\left.\begin{aligned}
F &= U_0V_0^T\\
F' &= JFJ,
\end{aligned}\right\} \tag{5.10}$$

where, for $l,\nu = 1, 2, \cdots,$

$$\left.\begin{aligned}
U_{l0} &= i^l\,(2l+1)\left[1+\frac{(l-1)(l+2)}{i2kd}\right]\\
V_{\nu 0} &= i^{-\nu}\,\nu(\nu+1)\left[1+\frac{\nu(\nu+1)}{i2kd}\right].
\end{aligned}\right\} \tag{5.11}$$

The coupled equations (2.8) become

$$\left.\begin{aligned} \Lambda^E(ka)A^E &= W_0 F B^E \\ \Lambda^H(ka)A^H &= W_0 F B^H \\ \Lambda^E(kb)B^E &= W_0 J F J A^E \\ \Lambda^H(kb)B^H &= W_0 J F J A^H \end{aligned}\right\} \tag{5.12}$$

Compare these with (3.12). As suspected, the coupling structure here is completely different from that for the cases $|m| \geq 1$. Here the electric multipoles from one sphere will couple only with electric multipoles of the other sphere, and similarly for the magnetic multipoles. This is obvious from the right hand side of each set of equations in (5.12) which, we recall, represents excitation from the opposite sphere. Thus the first and third sets of equations (electric) can be solved independently of the second and fourth (magnetic), yielding two distinct types of free oscillation for $m = 0$; there are no hybrid modes. Notice that this coupling structure obtains for *any* sphere separation, not just $d \to \infty$. [(5.1) implies $\mathbf{M}_{l0}^{(j)}$ and $\mathbf{M}'^{(j)}_{l0}$ have only a $\hat{\phi} = \hat{\phi}'$ component, so by (5.3) $\beta_{\nu 0}^{l0} = 0$ for all d]. The same cannot be said of (3.12).

At this point it is expedient to review some distinguishing properties of the electric and magnetic multipoles. The magnetic multipoles $\mathbf{M}$ do not have a radial component. Furthermore, with $m = 0$ $\mathbf{M}$ has only a $\hat{\phi}$ component. Thus the electric field of a magnetic free oscillation [(2.4) with $A^E = 0 = B^E$ and $m = 0$] has no field line terminating perpendicular to the surface of either conducting sphere, which implies no net surface charge. By the surface continuity equation we then conclude that the surface current is divergenceless; in particular, the lines of surface current form closed loops in the $\hat{\phi}$ direction only. On the other hand, the electric multipoles $\mathbf{N}$ have a radial component, so that the electric free oscillations are associated with a net surface charge (locally).

As already mentioned, the first and third set of equations of (5.12) correspond to the electric free oscillations. Making suitable substitutions we find

$$A^E = (Q^E)^N A^E, \tag{5.13}$$

which must be valid for any $N \in \{1, 2, ...\}$, and where the matrix

$$Q^E = (W_0)^2 \, [\Lambda^E(ka)]^{-1} \, FJ \, [\Lambda^E(kb)]^{-1} \, FJ. \tag{5.14}$$

Using (5.10) we find

$$(Q^E)^N = \left[(W_0)^2 \, \chi_0^E(ka) \, \chi_0^E(kb) \right]^{N-1} Q^E, \tag{5.15}$$

where the scalar

$$\chi_0^E(\zeta) = V_0^T \, J \, [\Lambda^E(\zeta)]^{-1} \, U_0 = \sum_{l=1}^{\infty} (-1)^{l+1} U_{l0} V_{l0} [\Lambda_l^E(\zeta)]^{-1} \tag{5.16}$$

$$= \sum_{l=1}^{\infty} (-1)^l \, (2l + 1) \, l(l + 1) \left[1 - \frac{i}{kd} \, [l(l + 1) - 1] \right] \frac{\partial_\zeta [\zeta j_l(\zeta)]}{\partial_\zeta [\zeta h_l^{(2)}(\zeta)]}$$

[see (5.11) and (2.8)]. (5.15) together with (5.13) imply the transcendental equation

$$[W_0(kd)]^2 \, \chi_0^E(ka) \, \chi_0^E(kb) = 1. \tag{5.17}$$

The second and fourth set of equations in (5.12) apply to the magnetic free oscillations. They differ from the electric case only formally by the interchange of superscripts $E \longleftrightarrow H$, and thus we need not repeat equations (5.13) to (5.17). Notice, however, that (5.16) becomes

$$\chi_0^H(\zeta) = \sum_{l=1}^{\infty} (-1)^l \, (2l + 1) \, l(l + 1) \left[1 - \frac{i}{kd} \, [l(l + 1) - 1] \right] \frac{j_l(\zeta)}{h_l^{(2)}(\zeta)} \tag{5.16'}$$

5.3 Natural Frequencies

In the limit $d \to \infty$ we write, in the usual notation,

$$\left.\begin{aligned} \chi_0^E(\zeta) \to \chi_0^{(0),E}(\zeta) &= \sum_{l=1}^{\infty} (-1)^l \ (2l+1)\ l(l+1)\ \frac{\partial_\zeta[\zeta j_l(\zeta)]}{\partial_\zeta[\zeta h_l^{(2)}(\zeta)]} \\ \chi_0^H(\zeta) \to \chi_0^{(0),H}(\zeta) &= \sum_{l=1}^{\infty} (-1)^l \ (2l+1)\ l(l+1)\ \frac{j_l(\zeta)}{h_l^{(2)}(\zeta)}. \end{aligned}\right\} \tag{5.18}$$

As in section 3.3 we can show that $\chi_0^{(0),E}(\zeta)$ and $\chi_0^{(0),H}(\zeta)$ are meromorphic functions; the poles, occurring exclusively in the upper half ζ-plane correspond directly to the set of electric and magnetic $m = 0$ natural frequencies of the singly sphere, respectively. The union of these two sets of poles is thus the same set encountered in the cases $|\, m \,| \geq 1$. Using (3.28) (which also applies for j_l) we obviously have

$$\chi_0^{(0)}(-\zeta^*) = [\chi_0^{(0)}(\zeta)]^*, \tag{5.19}$$

which applies for both electric and magnetic cases. Finally, as $d \to \infty$ $W_0(kd) \to \infty$ for k in the upper half plane, but vanishes elsewhere (except at the origin, where $\chi_0^{(0)}$ has a third order zero, with similar consequences as discussed in section 3.3). These facts, together with the transcendental equation (5.17) allow us to conclude that the upper half plane zeros of $\chi_0^{(0)}(\zeta)$ (which are all first order) are symmetrically disposed about the imaginary ζ-axis and furnish the $m = 0$ natural frequencies through (3.32). As usual we need only consider the case $a = b$.

We now use the first order information to determine the departure vectors. We write (5.16) in the form

$$\chi_0^E(\zeta) = \left[1 + \frac{i}{kd}\right] \chi_0^{(0),E}(\zeta) - \frac{1}{kd}\, \eta_0^E(\zeta) \tag{5.20}$$

where we have defined

$$\eta_0^E(\zeta) \equiv i \sum_{l=1}^{\infty} (-1)^l \ (2l + 1) \ [l(l + 1)]^2 \ \frac{\partial_\zeta[\zeta j_l(\zeta)]}{\partial_\zeta[\zeta h_l^{(2)}(\zeta)]} \tag{5.21}$$

which is completely independent of the previous η_m defined in (3.62). As usual we now set $k = k_0 + \Delta k$, where k_0 is a solution when $d \to \infty$, and find that in the large d limit

$$\Delta k a = \frac{1}{k_0 d} \ \frac{\eta_0^E(k_0 a)}{\chi_0^{(0),E\prime}(k_0 a)} = O\left[\frac{1}{k_0 d}\right]. \tag{5.22}$$

Notice that the departure vector is again independent of the parity of the natural mode ($a = b$).

For the magnetic case we simply replace the superscript E with H; (5.21) becomes

$$\eta_0^H(\zeta) \equiv i \sum_{l=1}^{\infty} (-1)^l \ (2l + 1) \ [l(l + 1)]^2 \ \frac{j_l(\zeta)}{h_l^{(2)}(\zeta)}. \tag{5.23}$$

For the purpose of calculating the departure vectors we find for the derivatives:

$$\left.\begin{aligned} \chi_0^{(0),E\prime}(\zeta) &= i \sum_{l=1}^{\infty} (-1)^l \ (2l + 1) \ l(l + 1) \ \frac{[1 - l(l + 1)\zeta^{-2}]}{[\partial_\zeta[\zeta h_l^{(2)}(\zeta)]]^2} \\ \chi_0^{(0),H\prime}(\zeta) &= i \sum_{l=1}^{\infty} (-1)^l \ (2l + 1) \ l(l + 1) \ \frac{1}{[\zeta h_l^{(2)}(\zeta)]^2} \end{aligned}\right\} \tag{5.24}$$

Figs. 7 and 8 display a few of the lower order $m = 0$ electric and magnetic natural frequencies and relative departure vectors. Again we stress that the right half plane zeros of $\chi_0^{(0),E}$ (the first layer, or perhaps only part of it) are *not* natural frequencies. Notice that $\chi_0^{(0),H}$ has no right half plane zeros. This is a curious difference between the two cases.

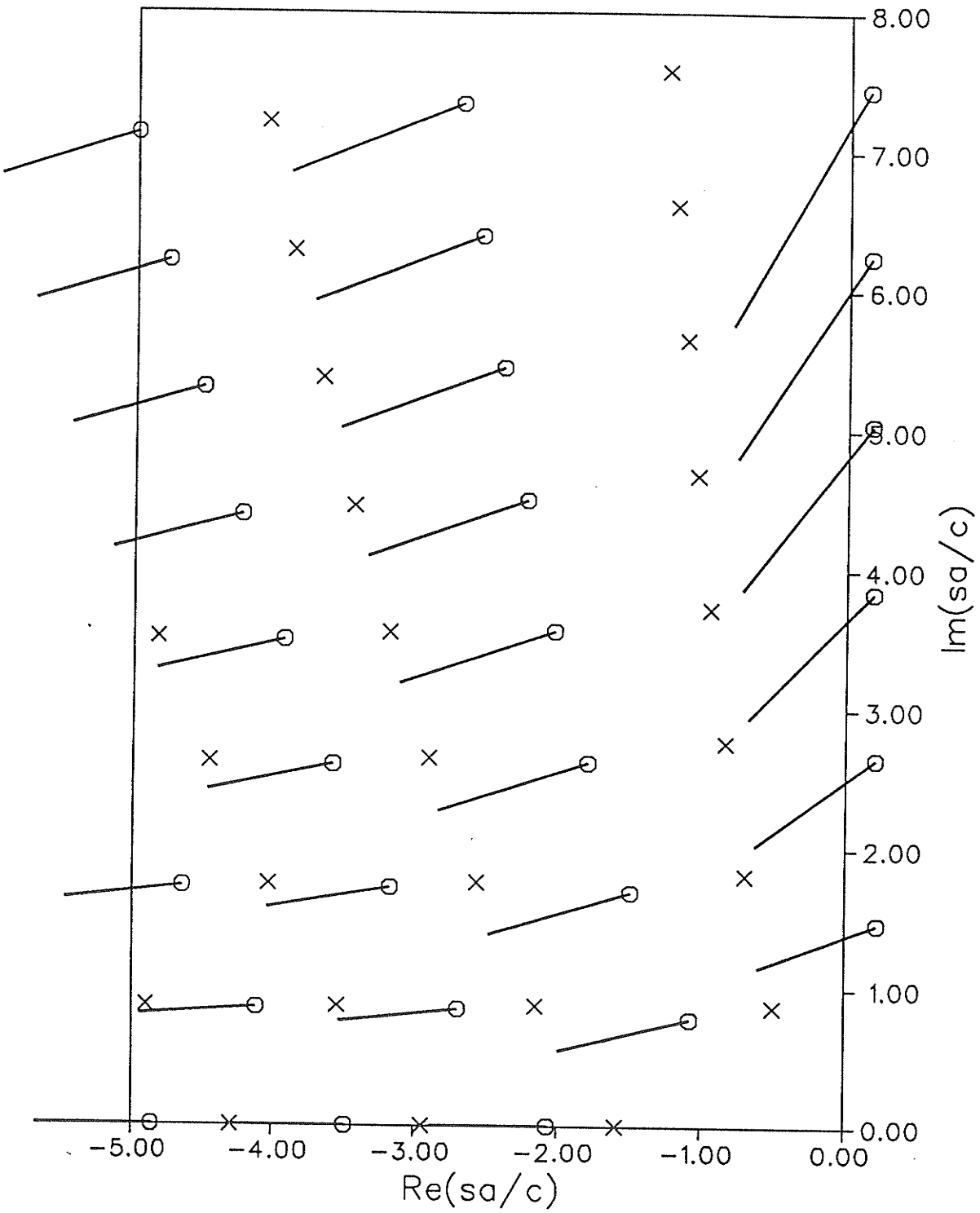

Fig 7: Natural frequencies and departure vectors for $d \to \infty$, a=b, m=0 electric type. For comparison the natural frequencies of a single sphere are indicated as $\times$(electric).

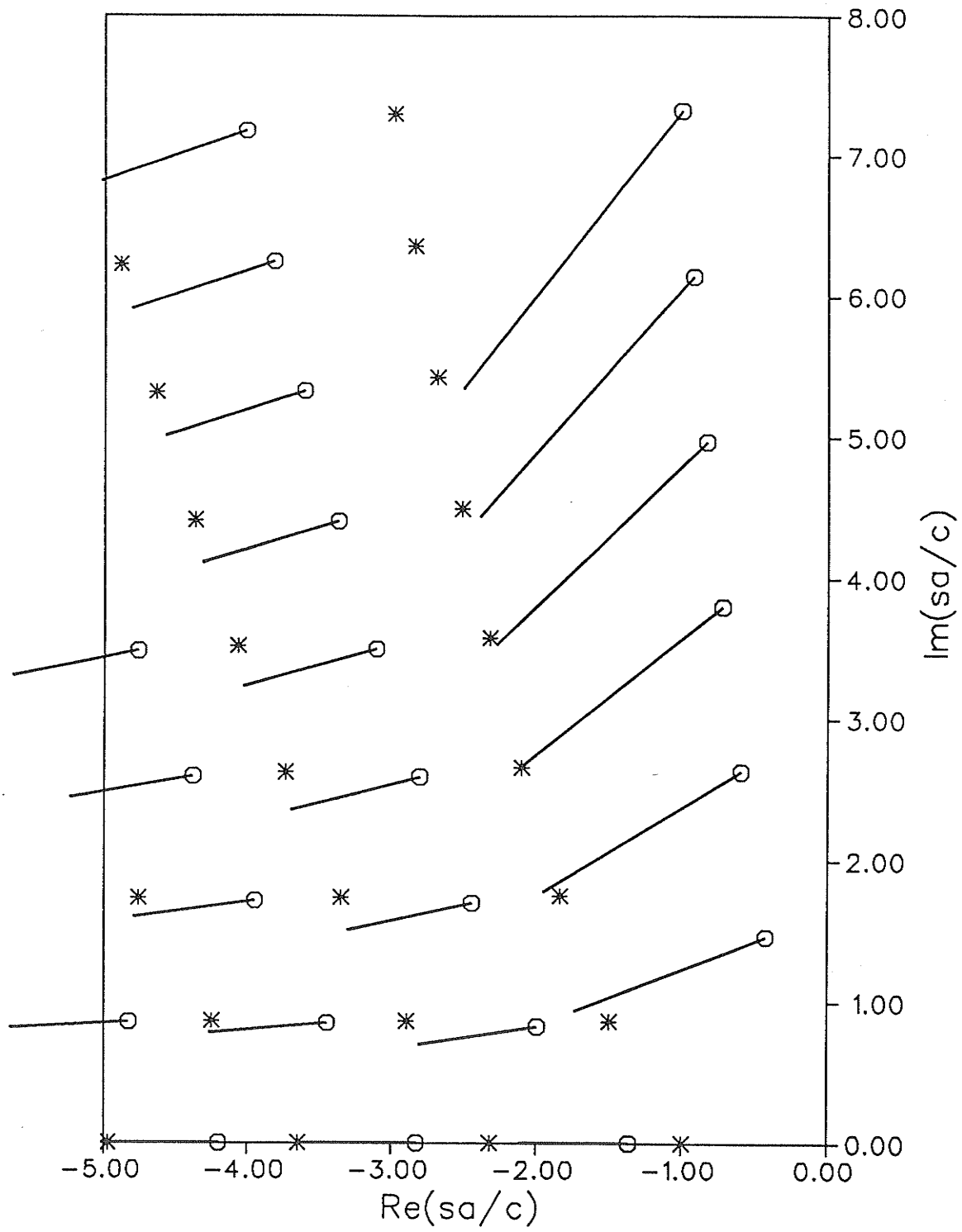

Fig 8: Natural frequencies and departure vectors for $d \to \infty$, a=b, m=0 magnetic type. For comparison the natural frequencies of a single sphere are indicated as $\ast$(magnetic).

In Fig. 7 we observe that the $m = 0$ electric natural frequency layers are "sandwiched" between the layers of electric natural frequencies of the single sphere (poles of $\chi_0^{(0),E}$), at approximately the location of the single sphere magnetic layers. This latter layer would represent poles, but are of course not present in the sum $\chi_0^{(0),E}$. Similar comments apply for the $m = 0$ magnetic natural frequencies in Fig. 8. This sandwiching of layers of zeros of χ between the single sphere pole layers behavior has already been observed in cases $|m| \geq 1$, see for example Fig. 2. We shall take up the discussion of the natural frequencies again in chapter 6.

5.4 Natural Modes

Starting with (5.13) (with $N = 1$) we find

$$A^E = \left\{ [W_0(kd)]^2 \, \chi_0^E(kb) \, V_0^T \, J \, A^E \right\} [\Lambda^E(ka)]^{-1} \, U_0. \tag{5.25}$$

B^E follows from (5.12). Setting the scalar in braces to unity yields

$$\left.\begin{aligned} A^E &= [\Lambda^E(ka)]^{-1} \, U_0 \\ B^E &= W_0(kd) \, \chi_0^E(ka) \, [\Lambda^E(kb)]^{-1} \, JU_0 \end{aligned}\right\} \tag{5.26a}$$

or to $W_0(kd) \, \chi_0^E(kb)$ yields the dual form

$$\left.\begin{aligned} A^E &= W_0(kd) \, \chi_0^E(kb) \, [\Lambda^E(ka)]^{-1} \, U_0 \\ B^E &= [\Lambda^E(kb)]^{-1} \, JU_0 \end{aligned}\right\} \tag{5.26b}$$

These are the $m = 0$ electric natural mode coefficients. Their (independent) magnetic counterparts are formally obtained by replacing superscript E with H. (Of course the

allowed values of k are determined from the set of electric or magnetic natural frequencies, respectively). Compare (5.26) with (3.45), which is very similar in form.

In the case $a = b$ the transcendental equation (5.17) implies

$$W_0(kd)\ \chi_0^E(ka) = p\,, \tag{5.27}$$

where $p = \pm 1$ marks parity as before. Then by (5.26a) the electric natural mode coefficients become

$$\left.\begin{aligned} A^E &= [\Lambda^E(ka)]^{-1}\ U_0 \\ B^E &= p\ [\Lambda^E(ka)]^{-1}\ JU_0, \end{aligned}\right\} \tag{5.28}$$

and similarly for the magnetic case. For all cases $|m| \geq 1$ $p = \pm 1$ indicated symmetric/antisymmetric natural modes. It turns out that the same rule applies for the magnetic $m = 0$ natural modes, but the converse rule must be used in the electric case. The proof runs along the same lines as in section 3.4.

The interaction fields for the electric natural modes are found from

$$\mathbf{E}_{B\to A}^{\text{inc}\,(E)} = \sum_{l=1}^{\infty} B_{l0}^E \mathbf{N}'^{(4)}_{l0} = \sum_{l=1}^{\infty} U_{l0}\mathbf{N}^{(1)}_{l0}. \tag{5.29}$$

The latter equality follows from using (5.28) and the matrix equations (5.12). This may be cast into a more explicit form by using (5.2b), namely

$$\mathbf{E}_{B\to A}^{\text{inc}\,(E)} = i\ (2\hat{z} - ik\rho\hat{\rho})\ e^{ikz}\ \left\{1 + \frac{1}{kd}\ \left[2kz + \frac{k^2\rho^2}{i2} + \times\hat{\phi}\ k\rho\right]\right\}. \tag{5.30}$$

Notice that on the axis this field has only a longitudinal component ($\hat{z}$). Perhaps our point is better illustrated by writing (5.30) in terms of spherical coordinates (about O'), namely

$$\mathbf{E}_{B\to A}^{\text{inc}\,(E)} = \left(\hat{\theta}' \frac{\sin\theta'}{2} + \hat{r}' \frac{i}{kr'} \right) \frac{1}{W_0(kd)} \frac{e^{-ikr'}}{kr'}. \tag{5.31}$$

The transverse component vanishes on the axis, allowing the longitudinal component to show itself as a first order correction. This is typical paraxial behavior for the electric field of an $m = 0$ electric multipole.

For the magnetic natural mode interaction fields we find the following various expressions:

$$\mathbf{E}_{B\to A}^{\text{inc}\,(H)} = \sum_{l=1}^{\infty} B_{l0}^{H} \mathbf{M}'^{(4)}_{l0} = \sum_{l=1}^{\infty} U_{l0} \mathbf{M}^{(1)}_{l0}. \tag{5.32}$$

$$= \hat{\phi}\, ik\rho\, e^{ikz} \left\{ 1 + \frac{1}{kd} \left[2kz + \frac{k^2\rho^2}{i2} \right] \right\}$$

$$= -\hat{\phi}'\, \frac{i\sin\theta'}{2} \frac{1}{W_0(kd)} \frac{e^{-ikr'}}{kr'}.$$

The magnetic interaction fields have only an azimuthal component which vanishes on the axis - typical paraxial behavior for the electric field of an $m = 0$ magnetic multipole.

In analogy with the $|m| \geq 1$ cases, the inverse $W_0(kd)$ is a direct manifestation of the destructive interference process, which tames the exponential growth in $e^{-ikr'}$.

It is interesting that $\mathbf{E}_{B\to A}^{\text{inc}\,(E)}$ and $\mathbf{E}_{B\to A}^{\text{inc}\,(H)}$ are duals of each other in the sense that

$$\left.\begin{aligned} \nabla \times \mathbf{E}_{B\to A}^{\text{inc}\,(E)} &= k\ \mathbf{E}_{B\to A}^{\text{inc}\,(H)} \\ \nabla \times \mathbf{E}_{B\to A}^{\text{inc}\,(H)} &= k\ \mathbf{E}_{B\to A}^{\text{inc}\,(E)}. \end{aligned}\right\} \tag{5.33}$$

This property follows directly from (5.29), (5.32), and (2.2). That this property holds for all sphere separation d should be obvious. [Actually the equality in (5.33) should be replaced with a proportionality sign since electric and magnetic $m = 0$ natural

modes are independent of each other. Furthermore, recall that the allowed values of k differ between electric and magnetic cases and so (5.33) is only *formally* correct.] Nevertheless it does illuminate how the coupling is related between electric and magnetic $m = 0$ free oscillations, and can also serve as a double-check in a numerical investigation.

CHAPTER 6: DISCUSSION AND CONCLUSION

In the previous chapters we discussed the free oscillations of the two-sphere geometry for large sphere separation. As directed by the equation structure we divided the discussion according to azimuthal dependence number m. Now we wish to unify and extend our understanding by considering the natural frequencies for all m values collectively, and try to identify or classify them according to possible relationships or correspondences with the single-sphere natural frequencies.

In Fig. 9 we have collected together a few of the lowest order natural frequencies for $|m| = 0, 1, 2, 3,$ and 4. We immediately notice a tendency of the natural frequencies to occur in groups, or clusters as we shall call them. A cluster is delineated by a closed dashed curve. We can label or identify the clusters by their layer number ($n = 0, 1, 2, \cdots$ beginning with the rightmost layer) and their arc number ($l = 1, 2, \cdots$ beginning with the arc closest to the origin). The layers and arcs form a grid with the clusters approximately at the nodes as sketched in the figure. The clusters become less compact as n decreases and l increases. We stress again that the zeros of $\chi_m^{(0)}$ in the right half s-plane are not natural frequencies, but have been included to display the pattern of zeros as clusters. Many transcendental equations have solutions where, for example, two functions intersect, or overlap; here we are interested in the intersection of the left half s-plane with the zeros of $\chi_m^{(0)}$. It just so happens that some of the zeros in the $n = 0$ clusters are excluded.

Except for the $n = 0$ layer, the ln^{th} cluster contains $2l + 1$ natural frequencies, including degeneracy over sign of m, i.e., includes cases $m = 0, \pm 1, \cdots, \pm l$. Let us denote these natural frequencies as $s_{ln}^{|m|}$, ln identifying the cluster and $|m| = 0, 1, \cdots, l$ identifying the natural frequency within that cluster. n even

(odd) indicates that the $m = 0$ natural frequency is of magnetic (electric) type. Notice that the $n = 0$ layer is not compatible with this classification scheme, and we temporarily ignore this special case (reserved for later discussion).

In Fig. 10 we show the first four arcs of electric and magnetic natural frequencies of a single sphere. As in Fig. 9 we label these arcs as $l = 1, 2, \cdots$ The layers are labeled with the index n again, but starting with $n = 1$ instead of $n = 0$. Then n even (odd) indicates a magnetic (electric) type of natural frequency as before. We denote these natural frequencies as s_{ln}. The lack of superscript $|m|$ emphasizes the degeneracy over m: A given s_{ln} corresponds to the natural modes $\mathbf{M}_{lm}^{(4)}(k_{ln}\mathbf{r})$ or $\mathbf{N}_{lm}^{(4)}(k_{ln}\mathbf{r})$ for $m = 0, \pm 1, \cdots, \pm l$, according to whether n is even or odd, respectively.

We now speculate that the single-sphere s_{ln} corresponds directly to the two-sphere $s_{ln}^{|m|}$ cluster (ignoring the $n = 0$ clusters). The nature of this correspondence and the reasons for its plausibility are now discussed. Consider for instance the $n = 2$ (magnetic) $l = 1$ (dipole) free oscillations of the single-sphere. The normalized natural frequency is $s_{12}a/c = -1 + i0$ and the natural modes are $\mathbf{M}_{1m}^{(4)}(k_{12}\mathbf{r})$ for $m = 0, \pm 1$ (3-fold degeneracy). Specialize further to the $m = 0$ case: $\mathbf{M}_{10}^{(4)}(k_{12}\mathbf{r}) = \hat{\phi}\, h_1^{(2)}(ir/a)\sin\theta$ is the electric field, which is symmetric with respect to reflection in the $z = 0$ plane. The surface current forms closed loops in the $\hat{\phi}$ direction and has functional dependence $\sin\theta$ - a magnetic dipole oriented in the $\hat{z}$ direction. Now suppose we continuously deform the sphere into a prolate spheroid, for example, or any other body symmetric under rotation in ϕ and reflection in the $z = 0$ plane. How will this change the natural frequency and the natural mode? Or, more importantly, what properties will remain invariant? We propose three intuitively obvious invariants: (i) parity (symmetric or antisymmetric under reflection in $z = 0$ plane), (ii) electric or magnetic type (applies only in $m = 0$ cases), and (iii) s on real axis (only

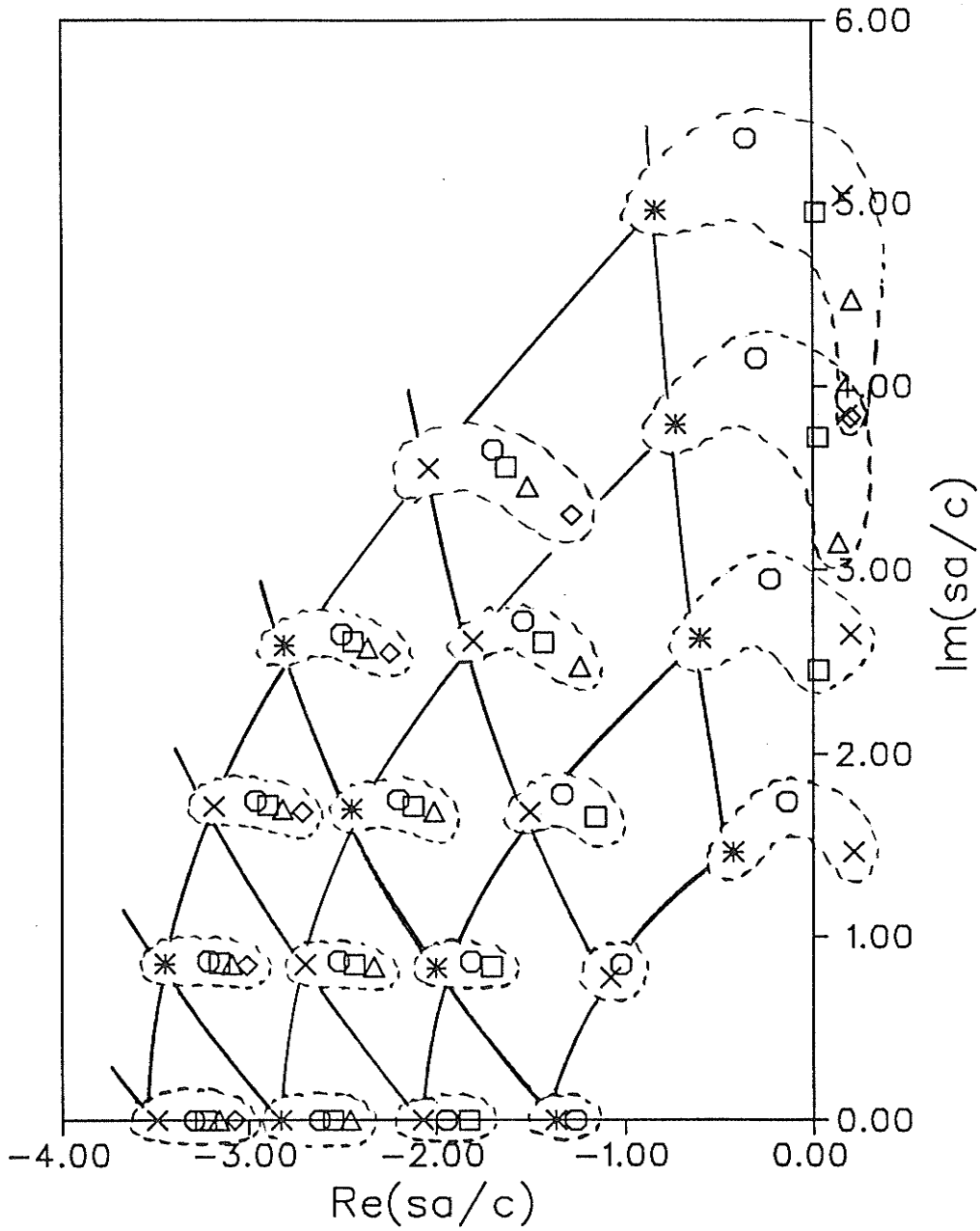

Fig 9: Natural frequencies for d→∞, a=b, cases:

×m=0 electric ○m=±1 △m=±3

✳m=0 magnetic □m=±2 ◇m=±4

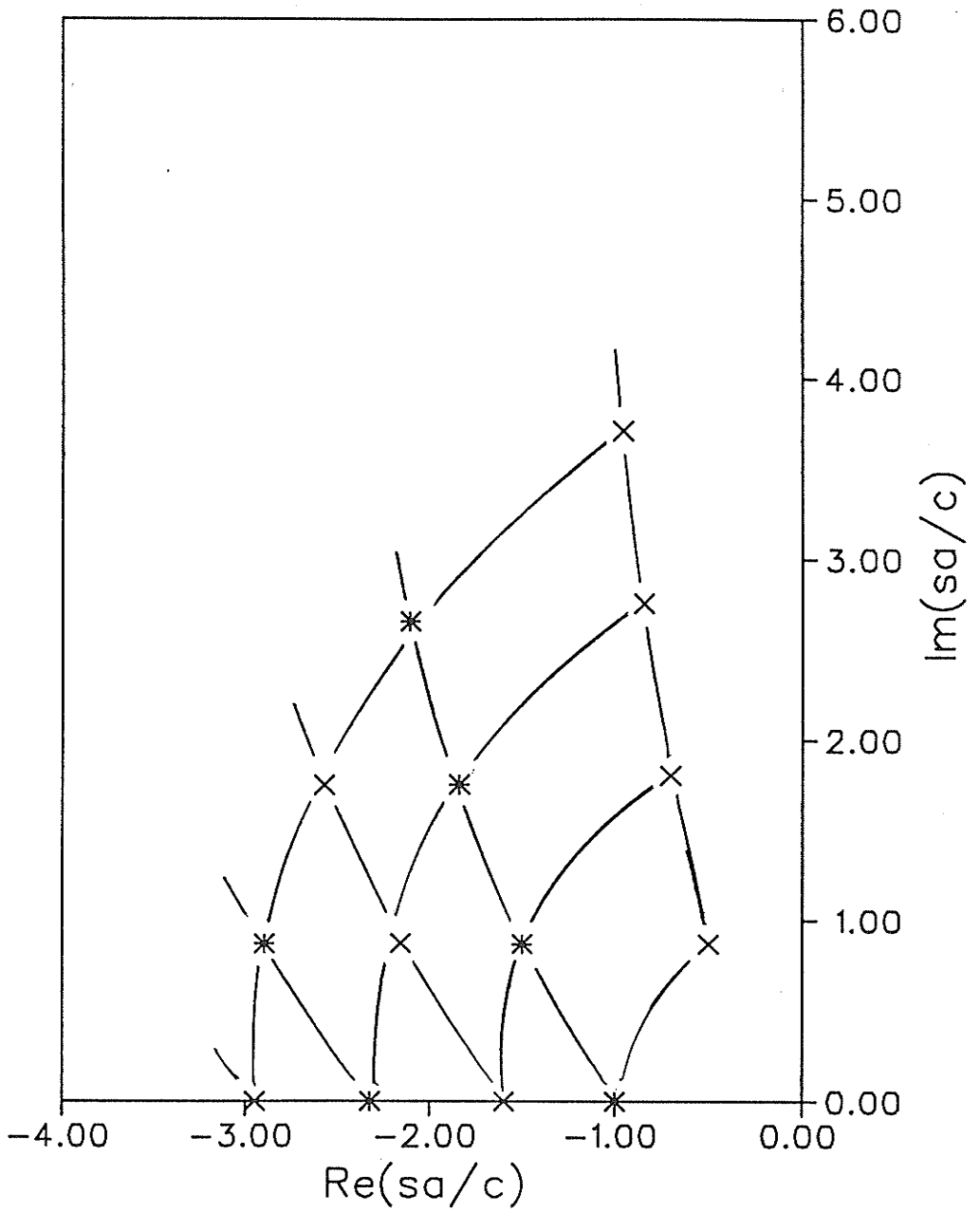

Fig 10: Natural frequencies of a single sphere.

× electric ✳ magnetic

for those that start on real axis).

Pertaining to the first property we notice that the new body (deformed sphere) is, by hypothesis, still symmetric under reflection in the z =0 plane and so the natural modes still have definite parity. It seems unlikely that a natural mode will suddenly flip from one parity to the opposite parity at some "critical object shape". We have not found any evidence to contradict this in any of the SEM literature. The invariance of type, electric or magnetic, for $m = 0$ free oscillations follows from the fact that the $m = 0$ electric and magnetic equations for any rotationally symmetric geometry decouple (are independent) [7]. We observed this phenomenon in section 5.2 where we found that the "decoupled structure" of (5.12) applies for any sphere separation. Finally, the idea that an s on the real axis will always remain on the real axis was discussed in section 3.7 in connection with the departure vector in (3.74). It also appears to apply, for example, for the prolate spheroid as the aspect ratio is varied, at least for the $m = 0$ electric free oscillations [7]. It seems plausible that this invariance is quite general, and we assume as much for the present discussion.

Now back to the magnetic dipole, $m = 0$ case: Suppose we continuously deform the sphere by pinching it around the equator until we have two identical, separated spheres. Then let the sphere separation $d \to \infty$. According to our invariances, the deformed natural mode will still be of $m = 0$ magnetic type (currents circulating in $\hat{\phi}$ direction), even parity, and s on the real axis. It is plausible that the s_{12}^0 natural frequency in Fig. 9 *is* that new s (compare with the original s_{12} in Fig. 10).

The remaining single-sphere natural modes belonging to s_{12} are the $\mathbf{M}_{1m}^{(4)}(k_{12}\mathbf{r})$ magnetic dipoles for $m = \pm 1$, which have odd parity. We expect the parity and "s on real axis" invariances to apply again, but since $m \neq 0$ the new natural modes should be hybrid. Furthermore, the cylindrical symmetry means that the degeneracy over sign of

m will not be lifted. Thus, as we deform the single-sphere into two identical infinitely separated spheres it is plausible that the single-sphere $m = \pm 1$ magnetic dipole modes deform into $m = \pm 1$ odd parity hybrid modes sharing the natural frequency s_{12}^{1} in Fig. 9. In summary, we are suggesting that as the single-sphere is deformed continuously into two identical infinitely separated spheres the s_{12} natural frequency in Fig. 10 splits into the $s_{12}^{|m|}$ cluster in Fig. 9, the degeneracy over $|m|$ having been lifted, with corresponding changes in the natural modes as discussed.

The same type of analysis can be applied to the other clusters on the real axis. Under the same geometry deformation, the $s_{l,l+1}$ natural frequency in Fig. 10 splits into the $s_{l,l+1}^{|m|}$ real axis cluster, where $|m| = 0, 1, \cdots, l$, the degeneracy over $|m|$ having been lifted. Also, the $m = 0$ types, electric or magnetic, of each cluster are correct. Furthermore, we observe that the $s_{l,l+1}^{|m|}$ cluster is always immediately to the left of its $s_{l,l+1}$ "origin", but always to the right of $s_{l+1,l+2}$, i.e., its extent is always confined to the real axis between two adjacent single-sphere natural frequencies. We propose that the real axis clusters may always be so constrained, regardless of sphere separation d; the exact coupled equations (2.8) always contain the factors $(\Lambda_l^E)^{-1}$ and $(\Lambda_l^H)^{-1}$ which are singular at the single-sphere electric and magnetic natural frequencies, respectively, and so the latter act as natural "barriers". Another way of thinking about it is to recall that the natural frequencies for any sphere separation cannot occur at (and thus avoid) single-sphere natural frequencies. This reasoning of course presupposes the constraint of the natural frequencies to the real axis, but it may also apply in a loose sense to all of the clusters, and may be related to the "sandwiching" behavior already discussed in previous chapters.

Inspection of both figures again suggests that this plausibility argument may be extended to all of the natural frequencies (except those in the $n = 0$ clusters): Under

the usual geometry deformation, the s_{ln} single-sphere natural frequency splits into the $s_{ln}^{|m|}$ cluster. The degeneracy over $|m|$ is properly accounted for as is the $m = 0$ type invariance (electric/magnetic). Notice that the parity invariance also applies, where $\mathbf{N}_{lm}^{(j)}$ has $(-1)^{l+m}$ parity and $\mathbf{M}_{lm}^{(j)}$ has $-(-1)^{l+m}$ parity under reflection in the $z = 0$ plane.

Thus we have a plausible theory connecting the single-sphere natural frequencies in Fig. 10 with those of the two-sphere problem in Fig. 9. This classification, or identification scheme accounts for all of the two-sphere natural frequencies and natural modes except for two prominent omissions. The first is the $n = 0$ layer of clusters which we have been ignoring, and the second involves (in the case $a = b$) the degeneracy over parity in Fig. 9 which we have carefully avoided discussing. Let us continue to ignore the $n = 0$ layer while addressing this latter problem first.

Recall that in the case $a = b$ and $d \to \infty$, equation (3.31) (and its counterparts for all m) imply that to every natural frequency in Fig. 9 (including degeneracy over sign of m) there corresponds *two* natural modes, one symmetric and the other antisymmetric under reflection in the symmetry plane. Apparently as $d \to \infty$ the natural frequencies coalesce in pairs corresponding to natural modes of opposite parity. Further evidence supporting this type of behavior for two-object geometries is found by Marin, mentioned in [4], Fig. 3.15, who considers two identical colinear cylinders. But when the single-sphere natural frequency s_{ln} splits into the two-sphere cluster $s_{ln}^{|m|}$, each natural frequency in the cluster (including degeneracy over sign of m) "should" correspond to only *one* natural mode, the parity of which comes from its single sphere origins according to our parity invariance property. But we observe exactly twice the number of natural modes than our theory can account for. In the more general case $a = b$ the parity degeneracy is lifted - the pairs split into two distinct natural

frequencies corresponding to the deformed symmetric (matched to smaller sphere) and deformed antisymmetric (matched to larger sphere) natural modes, as discussed in section 3.4. But we still can only account for half of these free oscillations; where do the rest come from?

At first thought the source of the problem may appear to be the double sign in (3.30). Analogous to many problems, perhaps only one choice of sign leads to a physically allowed solution and the other is to be ignored. But then for a given m all the natural modes would have the same parity - clearly this is unacceptable. Besides, when $a \neq b$ equations (3.42) clearly indicate a twofold set of solutions.

By examining the results in [7] it is clear that our theory *can* be applied successfully to the case of a sphere continuously deformed into a prolate spheroid (at least for the $m = 0$ electric free oscillations). It seems that our problem is unique to a *two*-object geometry. Thus we are led to propose the following explanation: In "continuously" deforming the single-sphere geometry into two separated spheres there is a discontinuous change in the set of allowed free oscillations - in particular, the number doubles over that expected from our earlier ideas. Naturally the point of discontinuity is when the single object separates into two.

To understand how this might come about on physical grounds consider two objects in contact at one point. For every allowed free oscillation, the electric potential must be the same at that point on both objects. Now separate the objects, even infinitesimally, and that constraint is removed; the system has acquired a new degree of freedom resulting in an increase in the number of allowed free oscillations. In terms of our two greatly separated spheres this new degree of freedom manifests itself as two possibilities: The natural frequency is either matched to sphere A or to sphere B. When $a = b$ these two possibilities become the degeneracy over parity. To test

this hypothesis further we have done some preliminary work on the three-sphere problem, which indicates that there may be at least a three-fold increase in the number of allowed free oscillations.

Thus we can now account for all of the free oscillations except those associated with the $n = 0$ layer of clusters in Fig. 9. Two general features make these clusters unique. Firstly they include *both* electric and magnetic $m = 0$ zeros of $\chi_0^{(0)}$ instead of just one or the other. Secondly only part of the zeros represent natural frequencies, the rest are in the right half plane. The first five clusters have only the $m = 0$ magnetic and $|m| = 1$ natural frequencies. The $|m| = 2$ natural frequencies are added for $l \geq 6$. Perhaps as l increases, higher $|m|$ natural frequencies are periodically added to the left half plane portion of the cluster. These unique features exclude these natural frequencies from our earlier classification scheme and lead us to suspect that their origins have a physically different explanation. Unfortunately, evidence of their origins does not survive the limiting process $d \to \infty$, even to first order. It is likely that they are again a phenomenon unique to multi-body geometries.

Let us digress for a moment to mention that the lifting of degeneracy over $|m|$ as a sphere is continuously deformed into another *single* cylindrically symmetric body has many examples in the SEM literature (see Moser *et al* [9]). Since cylindrical symmetry is the basic criterion, it should also apply for a *two*-body problem like two spheres, as we have observed here (with of course some features unique to the two-body geometry). [9] point out that this "radar spectroscopy", as he calls it, may be useful in radar target identification. An interesting extension of his work is to consider how, in general, the coupling between two known targets (like two spheres) changes the "radar spectrum" over that of the targets considered individually. Intensive analytical and numerical work should yield some basic physical insights. For example,

suppose it is true that the electric dipole free oscillations associated with the fuselages of two neighboring aircraft couple strongly (large changes in natural frequencies) because they have parallel polarization, but the fuselage-wing coupling can be neglected because the dipoles have perpendicular polarizations. Information like this can be used to understand or predict the radar spectrum of aircraft flying in formation. The present work represents some of the first steps in this direction. Especially useful might be the work of Cooray and Ciric [12]. They have found the rotational-translational addition theorem for two spheroids with arbitrary orientation. Perhaps the far field form of this theorem is suitable to make an investigation along the lines considered here feasible. It is easy to see how even a solution for far field separation can yield important information on how polarization affects mode coupling to change the radar spectrum.

We would also like to comment on the fact that due to causality the strength of coupling increases with increased sphere separation. This concerns the nature of the free oscillations themselves and has nothing to do with how strongly an incident field will couple to, or excite the various natural modes. This latter information comes from solving the conjugate adjoint, or transposed problem to find the so called coupling vectors (column matrices in a matrix formulation). There is a coupling vector associated with each natural mode which, when combined with the incident field data (direction, polarization, et cetera) yields the coupling, or excitation coefficient for that natural mode [4].

Let us conduct a thought experiment involving transient scattering from the two-sphere geometry. Consider an end-fire incident temporal delta function excitation striking sphere A first. This initially excites the "early- time" response of sphere A, which includes any response not representable as a constant coupling coefficient

superposition of (single-sphere) free oscillations. According to Morgan [13] the scattered field consists of a physical optics term and a mutual interaction term, the latter may be represented by a superposition using temporally varying coupling coefficients in the early-time (one possibility). But "after the traveling wave impulse has completed its transit of the body the scattered fields will be produced by undriven, source-free, current modes and can thus be represented by a simple class 1 [constant coupling coefficient] expansion in the late-time". Heyman and Felsen [14], on the other hand, feel that using temporally varying coupling coefficients in the early-time, although legitimate, is artificial and instead construct a self-consistent theory linking wavefront (GTD) analysis in the early-time with SEM (global resonances) in the late-time: "the analysis clarifies the evolution of resonances as collective summations of multiple wavefront fields which are caused by successive reflections or diffractions at the surfaces and scattering centers comprising the object". Either way, in general terms we may say that the free oscillations (global resonances) do not begin to dominate the scattering response until the driven response is past and all the elements of the distributed body have had a chance to mutually interact.

Now before the incident field strikes sphere B, sphere A is already entering the late-time phase. Then the incident impulse and the field forward scattered from sphere A excites sphere B. Notice that this does not simply excite the free oscillations of sphere B (as an incident impulse by itself would do) because such fields have zero tangential $\mathbf{E}$ and cannot satisfy the boundary conditions in light of the forward scattered field from sphere A. These latter fields drive sphere B at sphere A natural resonant frequencies, as does the impulse at all frequencies. After some time the fields backscattered from sphere B reexcite sphere A, and so on. Multiple such scattering events must eventually synthesize the global two-sphere free oscillations discussed in

this investigation. In fact, Morgan's [13] ideas should also be valid in the two-body case, which means that immediately after the impulse has passed sphere B, the scattered fields can be represented by a constant coefficient sum of the two-sphere free oscillations. The fact that one sphere is actually driving the other, and vice-versa, is no different from the interaction of currents via fields on different parts of a single body - as for any geometry, the two-sphere free oscillations are source free fields that satisfy the appropriate boundary conditions.

The main point is that multi-body problems amplify the mechanisms involved in the early-time dynamics. A multi-body problem is no different from a single-body problem except for heavy emphasis on causality conditions concerning interactions between various elements. The larger the separation between the bodies the longer the definition of early-time and the synthesis of global resonances.

The second point concerns the practicality of our free oscillations for large sphere separation d. Certainly if we place a detector in the vicinity of sphere A the effects of sphere B on any scattering process must vanish as $d \to \infty$: The early-time becomes so long (multiple scattering events become weaker and occur less frequently) that by the time free oscillations dominate the response (late-time) they have extremely small amplitude, i.e., as $d \to \infty$ not only do we have to wait an infinite time for the coupling coefficients to become operative, they also vanish. (It is also true that the largest of these coupling coefficients should be for $|m| = 1$ free oscillations). The global resonances exist for any geometry, however small their effect. Umashankar *et al* [10] makes the same observation concerning a finite wire above a parallel ground plane.

Some of the questions raised in this investigation might be answered by a detailed numerical solution of the original equations (2.8) when the spheres are in the near field of each other, and so this represents the next logical step. For example, how in detail

does the duplicity of free oscillations emerge as the two spheres, initially in contact, are separated? How do the $n = 0$ clusters arise? And so on. The present efforts should provide some guidelines to the basic principles behind, and physical interpretation of such a set of detailed numerical results. It also of course provides the exact solution in the limiting case $d \rightarrow \infty$ as a numerical accuracy reference. Then, with a complete understanding of the free oscillations, especially quantitative results for the spheres in close proximity, one can apply the SEM to study some transient scattering phenomena. This, and other obvious extensions, are left for future research.

REFERENCES

[1] J.A. Stratton, *Electromagnetic Theory*, McGraw Hill, New York, 1941.

[2] J.H. Bruning and Y.T. Lo, "Multiple scattering of EM waves by spheres part I - modal expansion and ray-optical solutions," *IEEE Trans. Antennas Propagat.*, vol. AP-19, May 1971, pp. 378-390.

[3] J.H. Bruning and Y.T. Lo, "Multiple scattering by spheres," Antenna Lab., Univ. Illinois, Urbana, Tech. Rep. 69-5, 1969.

[4] L.B. Felsen Ed., *Transient Electromagnetic Fields*, Springer-Verlag, New York, 1975. Chapter 3: C.E. Baum, "The singularity expansion method."

[5] C.E. Baum, "On the singularity expansion method for the solution of electromagnetic interaction problems," Interaction Note 88, Dec. 1971.

[6] E. Merzbacher, *Quantum Mechanics*, *Sec. Ed.*, John Wiley and Sons, New York, 1970.

[7] L. Marin, "Natural-mode representation of transient scattering from rotationally symmetric bodies," *IEEE Trans. Antennas Propagat.*, vol. AP-22, Mar. 1974, pp. 266-274.

[8] R.F. Harrington, *Time–Harmonic Electromagnetic Fields*, McGraw Hill, New York, 1961.

[9] P.J. Moser and H. Uberall, "Complex eigenfrequencies of axisymmetric perfectly conducting bodies: radar spectroscopy," *Proc. IEEE*, vol. 71, Jan. 1983, pp. 171-172.

[10] K.R. Umashankar, T.H. Shumpert, and D.R. Wilton, "Scattering by a thin wire parallel to a ground plane using the singularity expansion method," *IEEE Trans. Antennas Propagat.*, vol. AP-23, Mar. 1975, pp. 178-184.

[11] T.H. Shumpert and D.J. Galloway, "Finite length cylindrical scatterer near perfectly conducting ground - a transmission line mode approximation," *IEEE Trans. Antennas Propagat.*, vol. AP-26, Jan. 1978, pp. 145-151.

[12] M.F.R. Cooray and I.R. Ciric, "Electromagnetic wave scattering by a system of two spheroids of arbitrary orientation," *IEEE Trans. Antennas Propagat.*, vol. AP-37, May 1989, pp. 608-618.

[13] M.A. Morgan, "Singularity expansion representations of fields and currents in transient scattering," *IEEE Trans. Antennas Propagat.*, vol. AP-32, May 1984, pp. 466-473.

[14] E. Heyman and L.B. Felsen, "A wavefront interpretation of the singularity expansion method," *IEEE Trans. Antennas Propagat.*, vol. AP-33, July 1985, pp. 706-718.

[15] L. Marin, "Natural-mode representation of transient scattered fields," *IEEE Trans. Antennas Propagat.*, vol. AP-21, Nov. 1973, pp. 809-818.

[16] F.M. Tesche, "On the analysis of scattering and antenna problems using the singularity expansion technique," *IEEE Trans. Antennas Propagat.*, vol. AP-21, Jan. 1973, pp. 53-62.

[17] M.L. Van Blaricum and R. Mittra, "A technique for extracting the poles and residues of a system directly from its transient response," *IEEE Trans. Antennas Propagat.*, vol. AP-23, Nov. 1975, pp. 777-781.

[18] C.E. Baum, "Emerging technology for transient and broad-band analysis and synthesis of antennas and scatterers," *Proc. IEEE*, vol. 64, Nov. 1976, pp. 1598-1616.

[19] K.M. Chen and D. Westmoreland, "Radar waveform synthesis for exciting single-mode backscatters from a sphere and application for target discrimination," *Radio Science*, vol. 17, May-June 1982, pp. 574-588.

[20] L.S. Riggs and T.H. Shumpert, "Trajectories of the singularities of a thin wire scatterer parallel to a lossy ground," *IEEE Trans. Antennas Propagat.*, vol. AP-27, Nov. 1979, pp. 864-868.

[21] T.T. Crow, C.D. Taylor, and M. Kumbale, "The singularity expansion method applied to perpendicular crossed wires over a perfectly conducting ground plane," *IEEE Trans. Antennas Propagat.*, vol. AP-27, Mar. 1979, pp. 248-252.

[22] D.J. Riley, W.A. Davis, and I.M. Besieris, "The singularity expansion method and multiple scattering," *Radio Science*, vol. 20, Jan.-Feb. 1985, pp. 20-24.

[23] M.L. Van Blaricum and R. Mittra, "Problems and solutions associated with Prony's method for processing transient data," *IEEE Trans. Antennas Propagat.*, vol. AP-26, Jan. 1978, pp. 174-182.

[24] K.S. Kunz and J.F. Prewitt, "Practical limitations to a natural mode characterization of electromagnetic transient response measurements," *IEEE Trans. Antennas Propagat.*, vol. AP-28, July 1980, pp. 575-577.

APPENDIX: SOME LIMITING FORMS FOR LEGENDRE AND SPHERICAL HANKEL FUNCTIONS

Legendre Functions

Using the definition ($l = 0, 1, 2, \cdots$)

$$P_l^m(x) = \frac{1}{2^l l!}(1-x^2)^{m/2}\frac{d^{l+m}}{dx^{l+m}}(x^2-1)^l, \qquad m = 0, 1, \cdots, l \quad \text{(A.1)}$$

$$= P_l^{-m}(x), \qquad m = -1, -2, \cdots, -l$$

it is easy to derive the following limiting forms for small argument θ (and $m \geq 0$):

$$P_l^m(\cos\theta) = A_l^m \left[1 - C_l^m\theta^2 + O(\theta^4)\right]\theta^m \quad \text{(A.2)}$$

$$\frac{P_l^m(\cos\theta)}{\sin\theta} = A_l^m \left[1 - C'^m_l\theta^2 + O(\theta^4)\right]\theta^{m-1} \quad \text{(A.3)}$$

$$\partial_\theta P_l^m(\cos\theta) = A_l^m \left[m - C''^m_l\theta^2 + O(\theta^4)\right]\theta^{m-1} \quad \text{(A.4)}$$

where

$$A_l^m = \frac{1}{2^m m!}\frac{(l+m)!}{(l-m)!}$$

$$C_l^m = \frac{m}{6} + \frac{(l-m)(l+m+1)}{4(m+1)}$$

$$C'^m_l = \frac{(m-1)}{6} + \frac{(l-m)(l+m+1)}{4(m+1)}$$

$$C''^m_l = \frac{m(m-1)}{6} + \frac{l(l+m+2)(l+m+1)(l-m+1) - (l+1)(l-m)(l-m-1)}{4(m+1)(2l+1)}$$

For $\theta \to \pi$, we simply replace θ with $\pi - \theta$ on the right hand side of (A.2) to (A.4), A_l^m

with $(-1)^{l+m} A_l^m$ in (A.2) and (A.3), and A_l^m with $-(-1)^{l+m} A_l^m$ in (A.4).

Spherical Hankel Functions

Using the standard definition of the spherical Hankel function we write, for $| z | \gg l(l+1)/2$ (and $l = 0, 1, 2, \cdots$)

$$h_l^{(2)}(z) = i^{l+1} \frac{e^{-iz}}{z} \left[1 + \frac{l(l+1)}{i2z} + O\left(\frac{l^4}{| z |^2} \right) \right] \tag{A.5}$$

$$\frac{1}{z} \partial_z [z \; h_l^{(2)}(z)] = -i \; i^{l+1} \frac{e^{-iz}}{z} \left[1 + \frac{l(l+1)}{i2z} + O\left(\frac{l^4}{| z |^2} \right) \right]. \tag{A.6}$$

Regarding (A.5) it is understood that the $O(l^4/| z |^2)$ term vanishes for $l = 0$ or 1, whereas in (A.6) it vanishes only for $l = 0$.